https://doi.org/10.1093/plphys/kiad312 PLANT PHYSIOLOGY 2023: 193: 643–660

Plant Physiology®

Research Article

Carotenoid sequestration protein FIBRILLIN participates in CmOR-regulated β-carotene accumulation in melon

Xuesong Zhou,[1,2,3] Tianhu Sun,[2,4] Lauren Owens,[2] Yong Yang,[2] Tara Fish,[2] Emalee Wrightstone,[2,4] Andy Lui,[2,4] Hui Yuan,[2,4] Noam Chayut,[5,6] Joseph Burger,[5] Yaakov Tadmor,[5] Theodore Thannhauser,[2] Wangzhen Guo,[1,*] Lailiang Cheng[3] and Li Li[2,4,*]

1 State Key Laboratory of Crop Genetics & Germplasm Enhancement and Utilization, Nanjing Agricultural University, Nanjing 210095, China
2 Robert W. Holley Center for Agriculture and Health, USDA-ARS, Cornell University, Ithaca, NY 14853, USA
3 Horticulture Section, School of Integrative Plant Science, Cornell University, Ithaca, NY 14853, USA
4 Plant Breeding and Genetics Section, School of Integrative Plant Science, Cornell University, Ithaca, NY 14853, USA
5 Department of Vegetable Research, ARO, Newe Ya'ar Research Center, Ramat Yishay 30095, Israel
6 John Innes Centre, Norwich Research Park, Norwich, UK

*Authors for correspondence: ll37@cornell.edu (L.L.), moelab@njau.edu.cn (W.G.).
The authors responsible for distribution of materials integral to the findings presented in this article in accordance with the policy described in the Instructions for Authors (https://academic.oup.com/plphys/pages/General-Instructions) are Li Li (E-mail: ll37@cornell.edu) and Wangzhen Guo (moelab@njau.edu.cn).

Abstract

Chromoplasts are plant organelles with a unique ability to sequester and store massive carotenoids. Chromoplasts have been hypothesized to enable high levels of carotenoid accumulation due to enhanced sequestration ability or sequestration substructure formation. However, the regulators that control the substructure component accumulation and substructure formation in chromoplasts remain unknown. In melon (*Cucumis melo*) fruit, β-carotene accumulation in chromoplasts is governed by ORANGE (OR), a key regulator for carotenoid accumulation in chromoplasts. By using comparative proteomic analysis of a high β-carotene melon variety and its isogenic line *low-β* mutant that is defective in *CmOr* with impaired chromoplast formation, we identified carotenoid sequestration protein FIBRILLIN1 (CmFBN1) as differentially expressed. *CmFBN1* expresses highly in melon fruit tissue. Overexpression of *CmFBN1* in transgenic Arabidopsis (*Arabidopsis thaliana*) containing OR^{His} that genetically mimics *CmOr* significantly enhances carotenoid accumulation, demonstrating its involvement in CmOR-induced carotenoid accumulation. Both in vitro and in vivo evidence showed that CmOR physically interacts with CmFBN1. Such an interaction occurs in plastoglobules and results in promoting CmFBN1 accumulation. CmOR greatly stabilizes CmFBN1, which stimulates plastoglobule proliferation and subsequently carotenoid accumulation in chromoplasts. Our findings show that CmOR directly regulates CmFBN1 protein levels and suggest a fundamental role of CmFBN1 in facilitating plastoglobule proliferation for carotenoid sequestration. This study also reveals an important genetic tool to further enhance OR-induced carotenoid accumulation in chromoplasts in crops.

Introduction

Carotenoids are widely distributed in nature. In plants, carotenoids play vital roles in photosynthesis and photoprotection (Domonkos et al. 2013; Niyogi and Truong 2013). They supply precursors for the biosynthesis of phytohormones abscisic acid and strigolactones (Al-Babili and Bouwmeester 2015), for the production of fruit and flower aroma and flavor (Auldridge et al. 2006; Walter and Strack 2011), and for the formation of growth regulators and signaling molecules (D'Alessandro and Havaux 2019; Havaux 2020;

Received February 27, 2023. Accepted May 05, 2023. Advance access publication May 26, 2023

Moreno et al. 2021). Carotenoids also furnish many flowers, fruits, and vegetables with bright orange, yellow, and red colors (Yuan et al. 2015b; Hermanns et al. 2020). In human diets, carotenoids provide precursors for vitamin A biosynthesis and act as dietary antioxidants to reduce the risk of some chronic diseases, such as cancers, cardiovascular diseases, and age-related eye diseases (Fraser and Bramley 2004; Rao and Rao 2007; Fiedor and Burda 2014).

Carotenoid accumulation is a net result of biosynthesis, turnover, and stable storage in plastids (Cazzonelli and Pogson 2010; Li and Yuan 2013; Rodriguez-Concepcion et al. 2018; Sun et al. 2018; Sun et al. 2022a). Phytoene synthase (PSY) catalyzes the condensation of 2 geranylgeranyl diphosphate molecules to phytoene in the specific carotenoid biosynthesis pathway (Supplemental Fig. S1). Many factors and regulators have been shown to modulate PSY expression and activity (Toledo-Ortiz et al. 2010; Martel et al. 2011; Kachanovsky et al. 2012; Zhou et al. 2015; Alvarez et al. 2016; Welsch et al. 2018; Zhu et al. 2021; Sun and Li 2020; Zhou et al. 2022). Phytoene is converted into lycopene following a series of desaturation and isomerization by 4 enzymes. Cyclization of lycopene produces α- and β-carotene in 2 branches of the pathway. Subsequent oxygenation and epoxidation of the carotenes make xanthophylls (Moise et al. 2014; Nisar et al. 2015; Sun et al. 2020a). Various carotenoid cleavage oxygenases, nonspecific enzymes, and nonenzymatic oxidations break down carotenoids to give diverse apocarotenoids and affect carotenoid content (Beltran and Stange 2016; Sun et al. 2020a).

Plastids are the site of carotenoid biosynthesis and storage (Sun et al. 2018). Among various plastids, the carotenoid-accumulating chromoplasts are the organelles that possess a high capacity to synthesize, sequestrate, and store massive amounts of carotenoids, giving many horticulture crops their vivid colors (Yuan et al. 2015b; Hermanns et al. 2020). Various studies have shown the direct association of chromoplast development with carotenoid accumulation (Liu et al. 2004; Lu et al. 2006; Kolotilin et al. 2007; Galpaz et al. 2008; Yuan et al. 2015a; Chayut et al. 2017; Llorente et al. 2020; Sun et al. 2020b). In some cases, carotenoid accumulation is impaired without chromoplast formation even when a similar carotenoid metabolic flux is observed in the carotenoid accumulating and nonaccumulating tissues (Li et al. 2003; Chayut et al. 2015).

In chromoplasts, carotenoids are sequestered and stabilized in various suborganellar structures composed of lipids and proteins (Vishnevetsky 1999; Sun et al. 2018). Based on the pigment lipoprotein sequestration substructures, chromoplasts are classified into various types such as globular chromoplasts characterized by abundant plastoglobules and membranous chromoplasts typified by multilayer membrane structures (Egea et al. 2010; Li and Yuan 2013; Sun et al. 2018). The only known protein involved in carotenoid sequestration and storage within chromoplasts is termed FIBRILLIN (FBN) after fibrils, which was identified in red pepper (*Capsicum annuum*) fruit and documented in vitro (Newman et al. 1989; Deruere et al. 1994). A homolog of this chromoplast-specific carotenoid sequestration protein was later identified in cucumber (*Cucumis sativus*) flowers (Vainstein et al. 1994; Vishnevetsky et al. 1996). FBN expression has been shown to affect carotenoid content in transgenic tomato (*Solanum lycopersicum*) fruit/flowers, be associated with carotenoid accumulation in tomato *high-pigment 1* mutant, and correspond with chromoplast development (Leitner-Dagan et al. 2006; Simkin et al. 2007; Kilambi et al. 2013; Llorente et al. 2020; Morelli et al. 2022). FBNs are known as structural proteins of not only fibrils but also plastoglobules, the lipoprotein particles, of plastids (van Wijk and Kessler 2017).

Melon (*C. melo*) is an economically important crop, consumed globally. Melon fruit flesh color is an important commercial trait and can be classified into 3 groups: white, green, and orange (Chayut et al. 2015). The orange flesh phenotype results from β-carotene accumulation in chromoplasts, which is governed by ORANGE (CmOR) containing a unique histidine residue (Tzuri et al. 2015; Chayut et al. 2017). CmOR exerts dual functions in regulating β-carotene accumulation in melon flesh (Chayut et al. 2017). One is to posttranslationally regulate the PSY protein level and activity to modulate carotenoid biosynthesis as found in Arabidopsis (*Arabidopsis thaliana*) and sweet potato (*Ipomoea batatas*) (Zhou et al. 2015; Park et al. 2016). The other is to induce chromoplast formation for β-carotene storage as observed in orange curd cauliflower (*Brassica oleracea* L. var. *botrytis*) as well as a few other plants (Lu et al. 2006; Yuan et al. 2015a; Yazdani et al. 2019; Sun et al. 2021). However, the mechanism of the CmOR-induced chromoplast formation remains to be elucidated and the proteins associated with carotenoid sequestration in melon chromoplasts are unknown.

It has long been hypothesized that chromoplasts enable high levels of carotenoid accumulation by a mechanism of promoting sequestration substructure formation. Melon fruit contains globular chromoplasts with abundant plastoglobules as the sequestration substructure (Jeffery et al. 2012). To investigate how CmOR regulates chromoplast development and to identify the protein associated with carotenoid sequestration in melon chromoplasts for β-carotene accumulation, a high β-carotene accumulating melon variety (CEZ) and its isogenic line *low-β* mutant were selected for the investigation. The *low-β* mutant results from a *CmOr* nonsense mutation (*Cmor-lowβ*) that impairs chromoplast biogenesis, leading to low β-carotene accumulation in the mature fruit (Chayut et al. 2017). Our previous comparative transcriptome analysis reveals that a major transcriptomic change occurs only at the mature fruit stage (Chayut et al. 2021). By proteome profiling of the mature fruit of CEZ and *low-β* mutant, we found that CmFBN1 was present at a high level in CEZ. A functional study of CmFBN1 demonstrated its involvement in CmOR-induced carotenoid accumulation. CmOR physically interacted with and stabilized CmFBN1. Microscopic and subplastidial fractionation analyses reveal that CmFBN1 enhances the CmOR-triggered carotenoid accumulation via stimulating plastoglobule proliferation for carotenoid sequestration within chromoplasts. Our findings provide a mechanistic understanding of regulating carotenoid

sequestration substructure formation for carotenoid accumulation in chromoplasts.

Results

Cmor-lowβ gene in the *low-β* mutant

The melon variety CEZ gives orange flesh fruit at mature stage (Fig. 1A). The orange color results from β-carotene accumulation (Fig. 1B). The *low-β* mutant is isogenic with CEZ, isolated from the CEZ ethyl methanesulfonate (EMS) mutagenesis library (Chayut et al. 2017). In comparison with CEZ, the *low-β* fruit showed a notable difference in flesh color at mature stage (Fig. 1A) and contained a significantly low level of β-carotene (Fig. 1B). In addition, CEZ fruit contained low levels of phytoene, phytofluene, and ζ-carotene, while *low-β* had lutein with much less total carotenoids (Supplemental Fig. S2, A to E). Except for fruit flesh color, the *low-β* mutant does not exhibit any plant growth and fruit development variation from its isogenic CEZ under both fields (Chayut et al. 2017) and greenhouse growth conditions (Supplemental Fig. S2F).

The *low-β* mutant results from a nonsense mutation in the *CmOr* gene to give the *Cmor-lowβ* allele (Chayut et al. 2017). The nonsense mutation occurs in exon 4 of *CmOr* (Fig. 1C), introducing a premature stop codon and producing a truncated CmOR protein (Cmor-lowβ) (Fig. 1D; Supplemental Fig. S3A). Structural analysis of the CmOR and Cmor-lowβ proteins using the Phobius tool (Kall et al. 2007) revealed that Cmor-lowβ lacks the 2 putative transmembrane domains and the DnaJ-like Cys-rich zinc finger domain of CmOR (Fig. 1D; Supplemental Fig. S3B). Quantitative reverse transcription PCR (RT-qPCR) analysis showed significantly lower expression levels of *CmOr* in *low-β* compared with CEZ in all tissues examined (Fig. 1E).

Proteome profile comparison between CEZ and *low-β* fruit

To identify the proteins that potentially participate in the CmOR-regulated chromoplast development and carotenoid accumulation, proteomic profiling of fruit at mature stage of CEZ and *low-β* was carried out using tandem mass tag (TMT) labeling combined with liquid chromatography-mass spectrometry (LC-MS/MS) analysis. A total of 5,826 proteins were detected from 3 biological replicates of CEZ and *low-β* samples. Principal component (PC) analysis illustrated that the fruit samples contained a substantially different set of proteins in CEZ compared to *low-β* (Fig. 2A). Large numbers of proteins with significantly different abundances were visualized in the volcano plot (Fig. 2B), showing a great effect of loss of functional *CmOr* on fruit proteome profile. Among them, 309 proteins were found to be differentially abundant with ≥1.5-fold change ($P < 0.05$). There were 183 proteins that were significantly upregulated and 126 were downregulated in *low-β* vs CEZ (Fig. 2C; Supplemental Data Set 1).

To determine the biological relevance of the proteomic changes, Gene ontology enrichment analysis of these differentially abundant proteins at fruit maturity was carried out (Fig. 2D; Supplemental Data Set 2). Substantial enrichments in biological processes were those relevant to photosynthesis, light harvesting, and protein-chromophore linkage. The differentially expressed proteins were mainly localized in cellular compartments of chloroplast thylakoid membrane. The enriched proteins were predominantly chlorophyll binding in molecular functions.

Among these differentially abundant proteins, those related to metabolic pathways were most abundant based on Kyoto Encyclopedia of Genes and Genomes (KEGG) pathway analysis (Supplemental Fig. S4; Supplemental Data Set 3). Other groups were those associated with photosynthesis involved in photosystem and ATP synthase, followed by photosynthesis antenna proteins and carbon fixation. Proteins involved in these processes in the KEGG analysis are indicated in Supplemental Fig. S5.

The loss of CmOR function in *low-β* did not greatly affect carotenoid metabolic pathway gene expression (Supplemental Fig. S6) but caused dramatically reduced PSY protein level during fruit developmental stages (Chayut et al. 2017; Chayut et al. 2021). At fruit mature stage, PSY protein accumulation in CEZ is also very low as in the *low-β* mutant (Chayut et al. 2017). Many proteins involved in the carotenoid metabolism pathway were identified in the proteomics study. Most of the identified pathway enzyme proteins showed different abundances (Fig. 2E).

Identification of FBN1 as a potential pigment sequestering protein in chromoplasts of melon fruit

Many proteins were substantially reduced in abundance in *low-β* mutant (Supplemental Data Set 1). The functional relationships of these proteins to CmOR in carotenogenesis and chromoplast biogenesis remain to be elucidated. Among the top 10 downregulated proteins identified with lowest *P* values (Fig. 2F), MELO3C007423 that encodes a chromoplast-specific carotenoid-associated protein (CmFBN) stood out. This is because that fibrillin has been shown to be involved in carotenoid sequestration within chromoplasts in pepper fruit and cucumber flowers (Deruere et al. 1994; Vishnevetsky et al. 1996).

FBNs are often present as a protein family, which are highly conserved and widely distributed in plants (Singh and McNellis 2011; Kim and Kim 2022). By homology search, 18 potential CmFBNs were identified in the melon genome. Detailed analysis of these sequences for the conserved PAP_fibrillin domain revealed that 9 of them were true CmFBN proteins. A phylogenetic comparison of these 9 protein sequences with Arabidopsis FBNs placed them in different clades (Fig. 3A) and enabled them naming based on their sequence similarities to Arabidopsis FBNs. Further phylogenetic tree analysis of CmFBNs with FBN proteins from other plant species supported the fact that CmFNBs belonged to 9 distinct clades out of the eleven plant FBN family clades

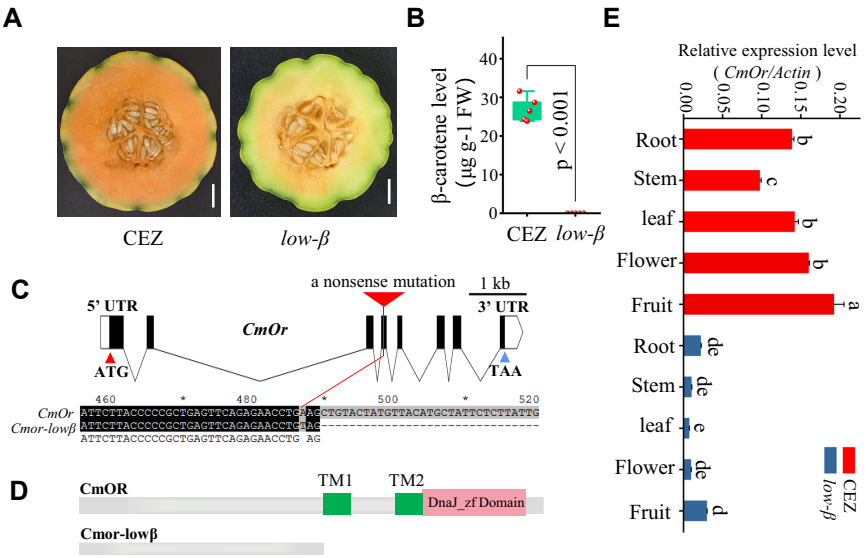

Figure 1. Characteristics of the *low-β* mutant. **A)** Phenotypes of CEZ and *low-β* mutant fruit at the mature stage. Scale bar 3 cm. **B)** β-carotene level in the flesh of mature fruit. Data are means ± SD of 5 biological replicates. Significant difference with $P < 0.001$ was analyzed by Tukey's test. **C)** Gene structure of *CmOr* and the nonsense mutation site in *Cmor-lowβ*. Exons are shown as black boxes. UTRs are shown as white boxes and introns are shown as lines. **D)** CmOR and Cmor-lowβ protein structures. Transmembrane domain (TM) and DnaJ zinc figure domain (DnaJ_zf domain). **E)** Expression level of *CmOr* in melon tissues by RT-qPCR. Data are means ± SE of 3 biological replicates. Different letters represent significant difference with $P < 0.05$, which was analyzed by Tukey's test. FW, fresh weight.

(Fig. 3B). MELO3C007423 cogrouped with those FNBs in clade 1, the group of FBNs associated with sequestration and storage of metabolites in plastids (Kim and Kim 2022), and therefore designated as CmFBN1. The others were highly divergent into other distinct clades (Fig. 3B). CmFBN1 shared sequence similarity (65.34% to 93.5%) with the chromoplast-specific carotenoid associated FBN proteins from bell pepper fruit and cucumber flower as well as an FBN protein in tomato fruit (Fig. 3C).

The digital expression of these *CmFBN* genes in various tissues of melon plants was examined based on expression data from melon genomics database (http://cucurbitgenomics.org/organism/18). While 6 of the *CmFBN* genes had relatively consistent low expression in nearly all tissues, 3 of them showed high levels of expression in specific tissues (Fig. 3D). *CmFBN3* is transcribed highly in roots and female flowers. *CmFBN6* is mainly expressed in leaves. *CmFBN1* is the only gene predominantly expressed in fruit as well as in male flowers (Fig. 3D). The expression pattern of *CmFBN1* was also confirmed by RT-qPCR (Fig. 3E). The high expression of *CmFBN1* in fruit tissue suggests its possible role in the CmOR-regulated chromoplast development and carotenoid accumulation in melon fruit.

Characterization of CmFBN1 gene and protein

The *CmFBN1* gene contains 3 exons (Fig. 4A) with 972 nucleotides and encodes 323 amino acids. While CEZ and *low-β* showed similar *CmFBN1* gene expression in roots, stems, leaves, and flowers, significant gene expression difference was observed in mature fruit by RT-qPCR analysis (Fig. 3E). To determine the developmental pattern of the *CmFBN1* expression during fruit ripening, we analyzed its digital expression at different fruit developmental stages based on our previous transcriptome data (Chayut et al. 2021). *CmFBN1* has the same transcript level in CEZ and *low-β* fruit at 10, 20, and 30 days after pollination (DAP) stages, but exhibits a significantly higher gene expression level in *low-β* than CEZ at the mature stage (Fig. 4B). Intriguingly, proteomic data revealed that CmFBN1 had a noticeably lower protein level in *low-β* than CEZ at the mature stage (Fig. 4C), suggesting a loss of stability of the CmFBN1 protein without functional CmOR in *low-β* fruit.

The subcellular localization of CmFBN1 in plant cells was examined. When CmFBN1-YFP fusion protein was expressed in *Nicotiana benthamiana* leaves, the YFP signal was found to localize to the plastids in the epidermal cells (Fig. 4D). We also examined the subcellular localization of CmOR and Cmor-lowβ. Both of them were located in the plastids of epidermal cells (Fig. 4D). Because Cmor-lowβ is truncated before its first transmembrane domain, it is expected that the truncation does not affect the subcellular localization of Cmor-lowβ protein.

FBN1 homologs were reported to be localized in plastoglobules of chromoplasts (Zeng et al. 2015). To examine whether CmFBN1 was also localized in plastoglobules, *CmFBN1-YFP* and a plastoglobule fluorescent protein marker *AtFBN4-mCherry* constructs were coinfiltrated in *N. benthamiana* leaves. A high magnification of chloroplasts in the mesophyll cells revealed that CmFBN1 was colocalized with the plastoglobule marker protein (Fig. 4E), indicating that CmFBN1 was localized in plastoglobules. The CmOR-

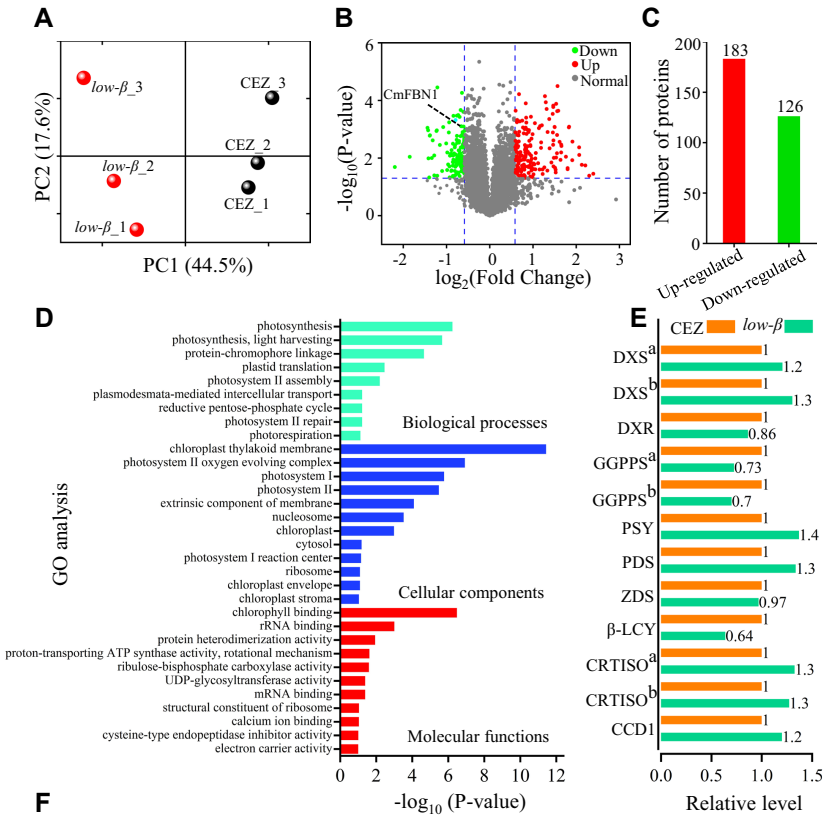

F

Accession	Protein Description	-log10 (P)
MELO3C016716.2.1	Fiber protein Fb34	4. 45
MELO3C015548.2.1	ARM repeat superfamily protein	4. 26
MELO3C013467.2.1	Transmembrane 9 superfamily member	3. 67
MELO3C010059.2.1	Zinc finger family protein	3. 61
MELO3C024407.2.1	Charged multivesicular body 1	3. 49
MELO3C015856.2.1	ELKS/Rab6-interacting/CAST family protein	3. 47
MELO3C003114.2.1	Mitochondrial ATP synthase 6 kDa subunit	3. 47
MELO3C024871.2.1	serine/threonine-protein phosphatase 4 regulatory subunit 2 isoform X1	3. 43
MELO3C007423.2.1	chromoplast-specific carotenoid-associated protein, chromoplastic	3. 32
MELO3C023644.2.1	subtilisin-like protease SBT3.17	3. 24

Figure 2. Proteomic profiling of differentially expressed proteins in CEZ vs *low-β*. **A)** PC analysis of total identified proteins from 3 biological replicates of CEZ and *low-β*. Results are presented based on correlation matrix in protein abundance. **B)** Volcano plot of proteins altered in *low-β* compared to CEZ. Red dots represent increased proteins, and blue dots represent decreased proteins with ≥1.5-fold change and $P < 0.05$. Gray dots represent proteins without significant changes in abundance. **C)** The number of up- and downregulated proteins in *low-β* vs CEZ at fruit mature stage. **D)** GO functional analysis of differentially expressed proteins. GO enrichment analysis was retrieved using DAVID. Top 10 significantly enriched GO (−log10 [*P*-value]) terms in biological process, molecular function, and cellular component branches are presented. All the adjusted statistically significant values of the terms were negative 10 base log transformed. **E)** Relative levels of carotenoid biosynthetic enzyme proteins in CEZ and *low-β*. **F**) The top 10 downregulated proteins in *low-β* compared to CEZ with lowest *P*-value at fruit mature stage. GO, gene ontology.

YFP signals appeared to be more uniformly distributed in chloroplasts (Fig. 4E).

CmFBN1 physically interacts with CmOR in plastids

In our previous study, we performed co-immunoprecipitation (co-IP) in conjunction with MS/MS analysis using proteins from Arabidopsis transgenic plants expressing OR-GFP to identify the OR-interacting proteins (Yuan et al. 2021). By searching the data, an Arabidopsis FBN protein was identified from the co-IP experiment, which guided us to investigate whether CmFBN1 physically interacts with CmOR to be involved in the CmOR-regulated β-carotene accumulation in chromoplasts in melon fruit.

We initially performed yeast 2-hybrid (Y2H) analysis. When CmOR-Nub and CmFBN1-Cub were coexpressed in yeast, yeast grew well on the selective medium (Fig. 5A). In contrast, little growth was observed when CmOR or CmFBN1 was coexpressed with empty vectors in the negative controls (Fig. 5A). We also investigated the interaction between CmFBN1 and Cmor-lowβ. The yeast growth was not observed in the selective medium (Fig. 5A), showing no interaction between CmFBN1 and Cmor-lowβ. The interaction strength in yeast was quantified by β-galactosidase activity assay. While the negative controls showed low β-galactosidase activity, the interaction between CmOR and CmFBN1 gave significantly high activity (Fig. 5B).

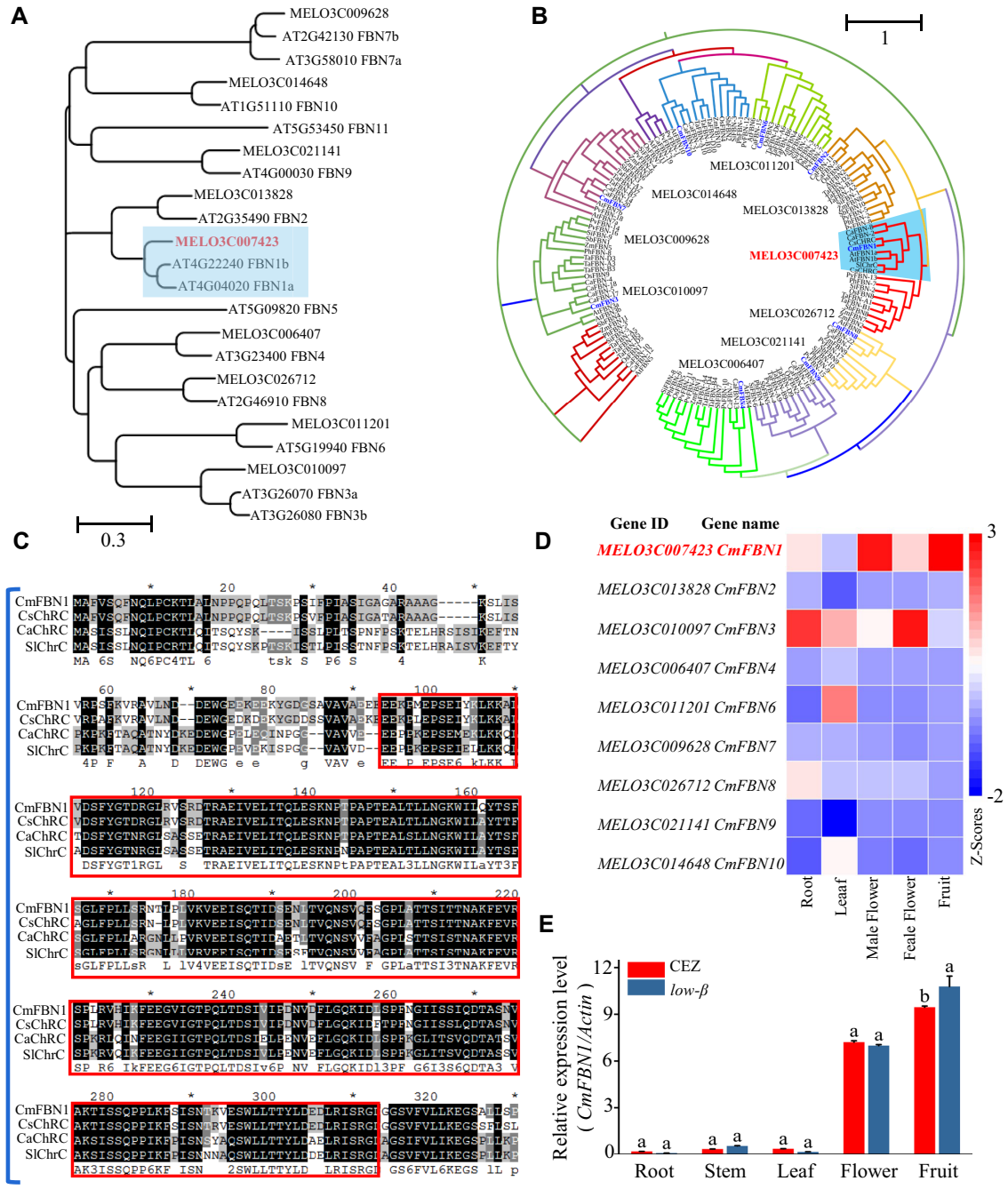

Figure 3. Phylogenetic analysis of CmFBNs and their expression patterns. **A)** Evolutionary relationship of FBNs from melon and Arabidopsis. The phylogenetic tree was performed using the neighbor-joining method. Bootstrap values were obtained from 1,000 bootstrap replicates. The scale bar shows 0.03 change per nucleotide. **B)** Phylogenetic analysis of FBNs from melon (*Cucumis melo*), Arabidopsis, wheat (*Triticum aestivum*), rice (*Oryza sativa*), tomato (*Lycopersicon esculentum*), pepper (*Capsicum annuum L.*), and cucumber (*C. sativus*). The phylogenetic tree was performed using the neighbor-joining method. Bootstrap values were obtained from 1,000 bootstrap replicates. The scale bar shows 1 change per nucleotide. **C)** Alignment of the FBN1 proteins from melon, cucumber, pepper, and tomato. Boxed is PAP_fibrillin domain. **D)** Heatmap of *CmFBN* expression patterns in different tissues of melon based on data from Cucurbit Genomics Database (http://cucurbitgenomics.org/organism/18). **E)** Expression levels of *CmFBNs* in different tissues of CEZ and *low-β* by RT-qPCR. Results are means ± SEM from 3 biological replicates. Different letters represent significant difference with $P < 0.05$, which was analyzed by Tukey's test.

To further confirm the interaction and observe the subcellular location of the interaction, bimolecular fluorescence complementation (BiFC) assay was performed. When CmOR-nYFP and CmFBN1-cYFP were coexpressed in *N. benthamiana* leaves, strong YFP signals were observed in the plastids of epidermal cells (Fig. 5C). In contrast, no signals were observed when Cmor-lowβ-nYFP and CmFBN1-cYFP were coexpressed (Fig. 5C), confirming no interaction between them as observed in Y2H. No signals were detected in the negative controls when CmOR-nYFP and cYFP vector only or nYFP only and

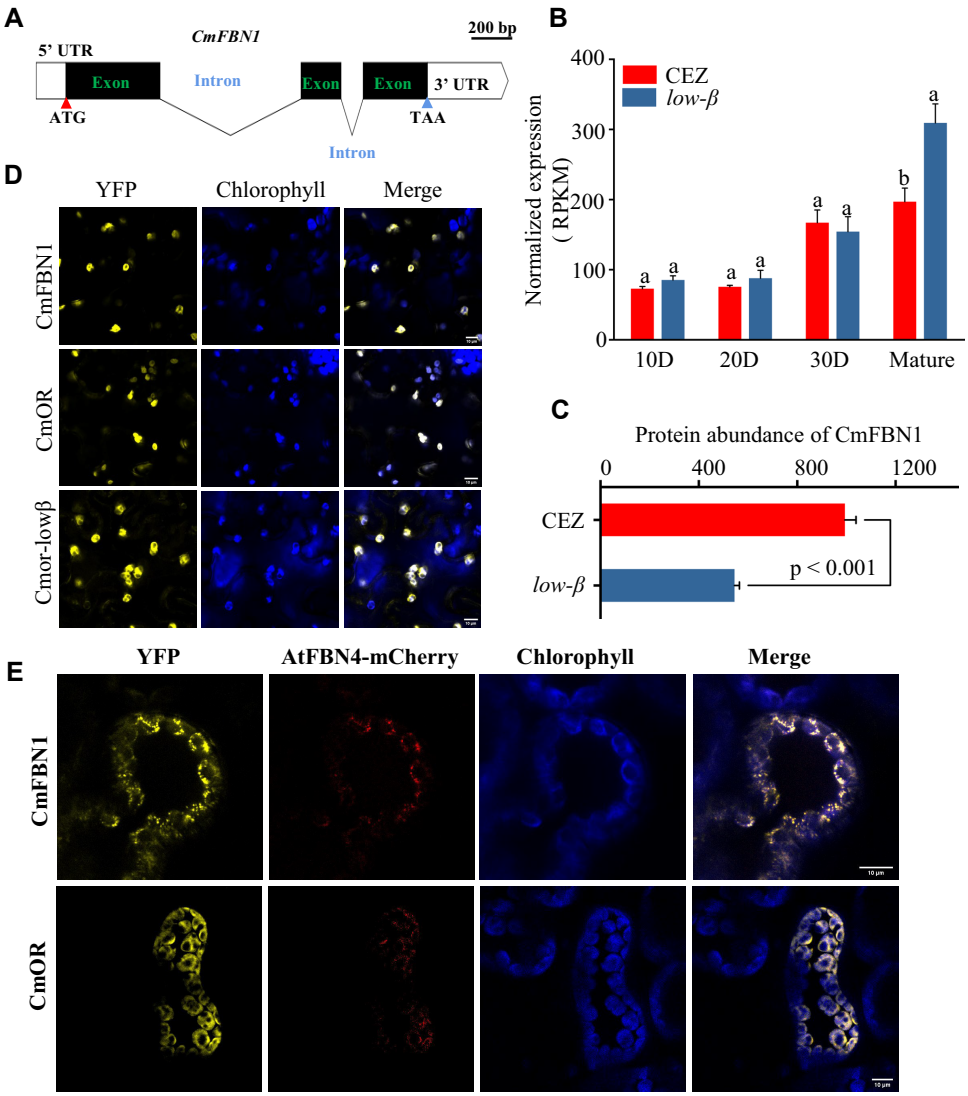

Figure 4. Characterization of CmFBN1 gene and protein. **A)** Gene structure of *CmFBN1*. **B)** Digital expression level of *CmFBN1* in CEZ and *low-β* based on data from Chayut et al. (2021). Bars represent average reads per kilobase of transcript per million mapped reads (RPKM) ± SE of 3 independent biological repeats. Different letters represent significant difference with $P < 0.05$, which was analyzed by Tukey's test. **C)** Protein level of CmFBN1 in CEZ and *low-β* in mature fruit based on the proteomic data. Results are means ± SEM from 3 biological replicates. Significant difference with $P < 0.001$ was analyzed by Tukey's test. **D)** Subcellular localization of CmFBN1, CmOR, and Cmor-lowβ in *N. benthamiana* leaf epidermal cells under confocal microscope. **E**) Subcellular localization of CmFBN1 and AtFBN4-mCherry in tobacco mesophyll cells under confocal microscope. Scale bar = 10 μm in **D** and **E**. YFP, yellow fluorescence protein.

CmFBN1-cYFP were coexpressed (Supplemental Fig. S7). While CmFBN1 is the only CmFBN that expresses highly in fruit tissue (Fig. 3D), we also examined whether CmFBN2 and CmFBN3 that express highly in leaf and flower/root tissues, respectively, physically interacted with CmOR by BiFC assay. No interactions were observed (Supplemental Fig. S8). Taken together, these data suggested that CmFBN1 and CmOR physically interact with each other in the plastids for carotenoid accumulation in melon fruit. In contrast, Cmor-lowβ lost the ability to interact with CmFBN1.

Noticeably when CmOR-nYFP and CmFBN1-cYFP interacted, strong YFP signals were localized in specific speckles in the epidermal cells (Fig. 5C), suggesting a plastoglobule localization. Thus, we coexpressed *CmOR-nYFP* and *CmFBN1-cYFP* with the plastoglobule fluorescent protein marker *AtFBN4-mCherry*. As shown in Fig. 5, D to E, interaction between CmOR and CmFBN1 resulted in the YFP signals that were colocalized with the plastoglobule marker protein in the chloroplasts of mesophyll cells. A high magnification view clearly showed many plastoglobules as dots with overlapped signals in the chloroplasts (Fig. 5E). These results indicate that CmOR was localized in the plastoglobules of chloroplasts when CmFBN1 was present.

CmFBN1 enhances carotenoid accumulation in the OR^{His} calli

In order to investigate whether *CmFBN1* has a role in the CmOR-regulated carotenoid accumulation, we first attempted

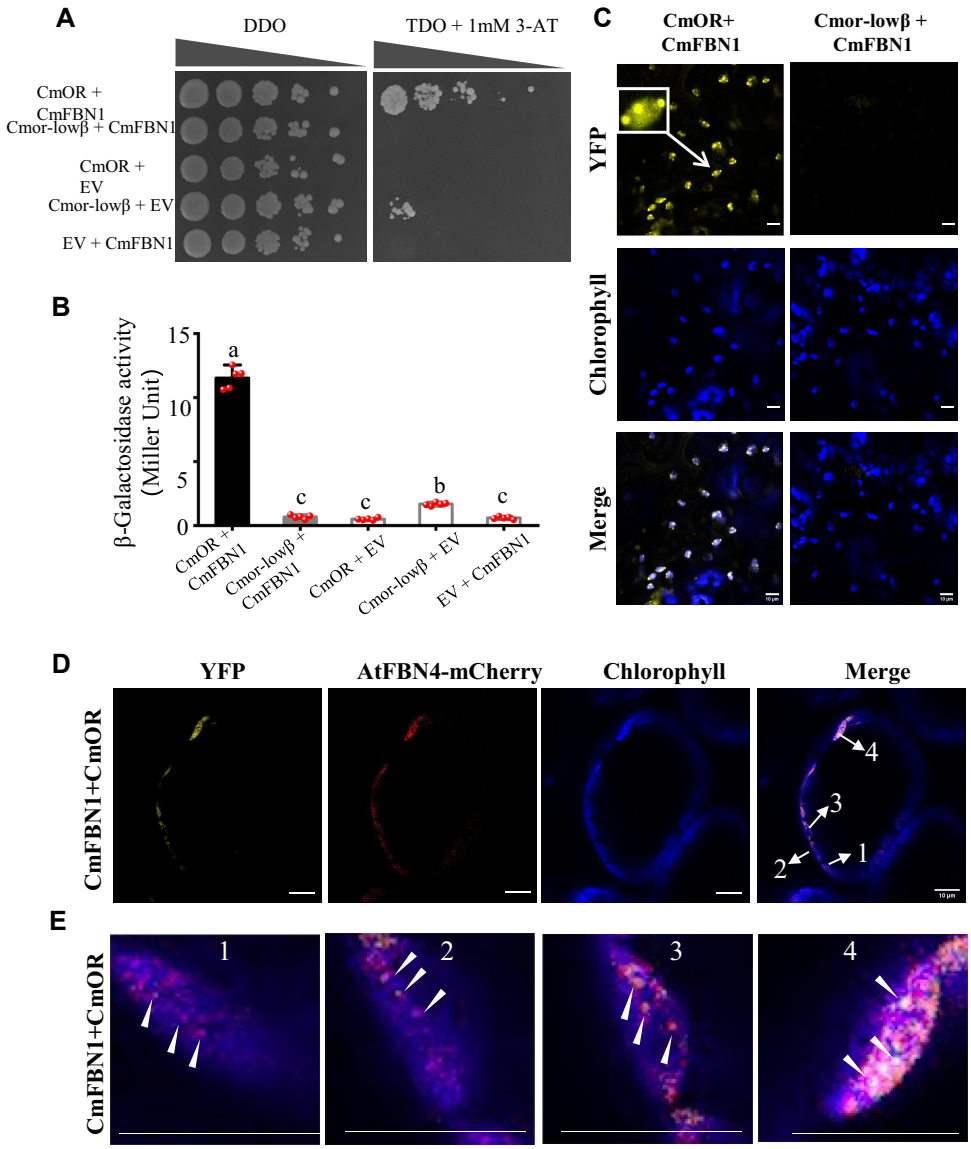

Figure 5. CmFBN1 physically interacts with CmOR in plastids. **A)** Y2H analysis. Yeast was spotted onto either nonselective drop-out medium without leucine and tryptophan (DDO) or selective medium lacking leucine, tryptophan, and histidine (TDO) plates with 1 mM 3-amino-1,2,4-triazole (3-AT) in a series of 10-fold dilutions. **B)** β-galactosidase activity. Bars represent the means ± SD calculated from 5 independent biological replicates with $P < 0.05$, which was analyzed by Tukey's test. **C)** BiFC analysis of CmOR-CmFBN1 and Cmor-lowβ-CmFBN1 interactions in *N. benthamiana* leaf epidermal cells under confocal microscope. CmFBN1 was fused with the C-terminus of YFP, whereas CmOR and Cmor-lowβ were fused with the N-terminus of YFP. Inset represents an enlarged plastid. **D)** Coexpression of CmFBN1-cYFP, CmOR-nYFP, and AtFBN4-mCherry in tobacco mesophyll cells under confocal microscope. **E)** Magnification of 4 merged chloroplast images in **D**. Arrows point to some representative plastoglobules. All scale bar sizes for **C**, **D**, and **E** are 10 μm.

the virus-induced gene silencing of *CmFBN1* in the CEZ melon fruit. The experiment was technically unsuccessful in our hands. We then performed the study by overexpression of *CmFBN1* in the background of Arabidopsis Col-0 wild type and OR^{His}, an Arabidopsis transgene genetically mimicking *CmOr* to induce chromoplast biogenesis in callus cells (Yuan et al. 2015a, 2015b). Three independent homozygous lines in each background were obtained. Noticeably, *CmFBN1* transgene had comparable expression levels in *CmFBN1* OR^{His} #2 and #5 lines as in the *CmFBN1* #1 line (Fig. 6A). We also examined *OR* expression in these transgenic lines. While reduced expression of *OR* was observed in the *CmFBN1* OR^{His} #1 and #5 lines, the other line #2 had similar *OR* expression level as the OR^{His} background (Fig. 6B). As expected, the Col-0 control and *CmFBN1* lines in the Col-0 background had low transcript levels of *OR* (Fig. 6B).

Since the OR^{His}-induced chromoplast biogenesis in Arabidopsis is only observed in callus cells (Yuan et al. 2015a) and callus is very responsive to increased carotenoid accumulation (Maass et al. 2009), we examined carotenoid accumulation in seed-derived calli from wild type control and those transgenic lines. The calli from the OR^{His} line

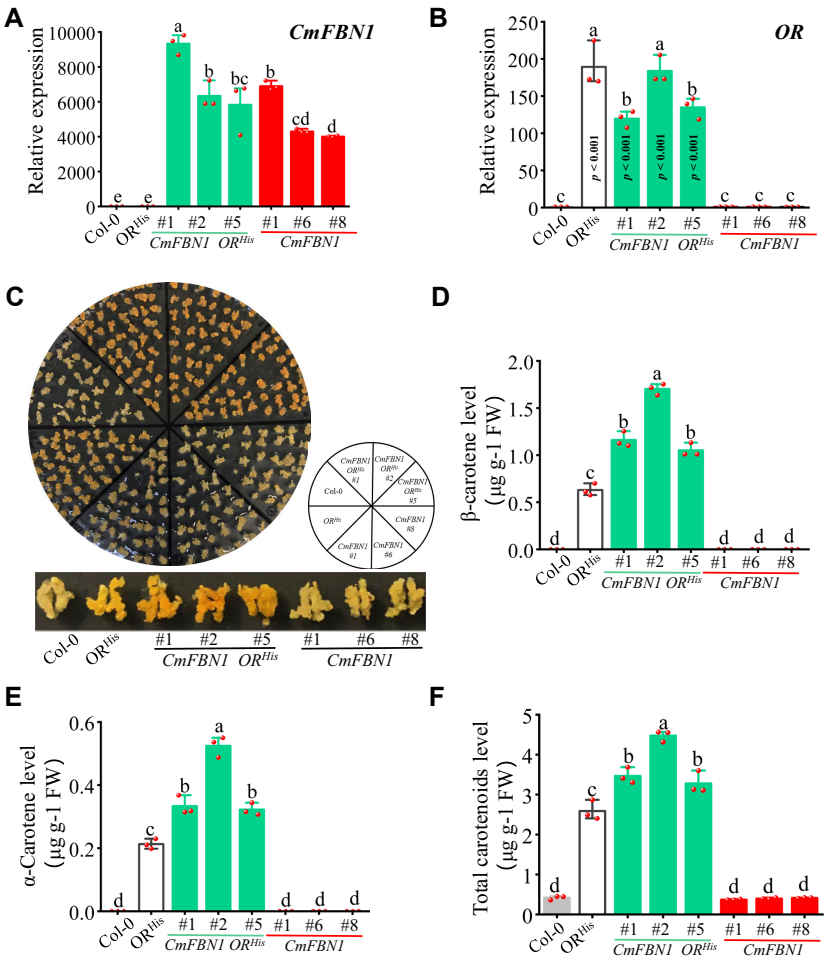

Figure 6. Coexpression of *CmFBN1* and OR^{His} that genetically mimics *CmOr* enhances carotenoid accumulation in Arabidopsis calli. **A)** Relative expression level of *CmFBN1* in Col-0 and transgenic lines by RT-qPCR. **B)** Relative expression level of *OR* in Col-0 and transgenic lines by RT-qPCR. **C)** Phenotypes of calli from various lines. **D)** β-carotene level. **E)** α-carotene level. **F)** Total carotenoid level. Carotenoid levels in calli were determined by UPC[2]. Results for all bar figures are means ± SEM from 3 biological replicates. Different letters represent significant difference with $P < 0.05$, which was analyzed by Tukey's test. FW, fresh weight.

showed a distinct orange color in comparison with those from Col-0 wild type control (Fig. 6C). The 3 *CmFBN1* OR^{His} lines gave a more intense orange color than the OR^{His} line, while the 3 *CmFBN1* lines in Col-0 background showed similar callus color as the wild type control (Fig. 6C). As a result, up to 2.71-fold higher level of β-carotene was detected in the *CmFBN1* OR^{His} lines than the OR^{His} line (Fig. 6D). The *CmFBN1* OR^{His} lines also produced up to 2.46- and 1.73-fold higher amounts of α-carotene and total carotenoids than the OR^{His} line, respectively (Fig. 6, E and F) with a similar level of lutein (Supplemental Fig. S9). The individual and total carotenoid content were found no significant differences between Col-0 control and the *CmFBN1* lines (Fig. 6, D to F). No consistently significant increase in the expression of carotenogenic genes was observed following the *CmFBN1* expression among those *CmFBN1* OR^{His} transgenic lines in comparison to Col-0 and OR^{His} (Supplemental Fig. S10). Since the OR^{His} line induces chromoplast formation in the calli whereas the Col-0 wild type control does not (Yuan et al. 2015a), these results showed that *CmFBN1* further enhanced the OR^{His}-regulated carotenoid accumulation in the presence of chromoplasts, but exhibited no dramatic effect on carotenoid accumulation by itself in the absence of chromoplast development.

We also examined the levels of other isoprenoid compounds, i.e. ubiquinone-10, α-tocopherol, and δ-tocopherol in the calli of these transgenic lines. No consistently significant changes in these metabolites were observed among wild type, OR^{His}, *CmFBN1* OR^{His}, and *CmFBN1* lines (Supplemental Fig. S11).

Plastoglobule proliferation in the *CmFBN1* OR^{His} lines

To examine the effects of *CmFBN1* expression on carotenoid accumulation structures in the *CmFBN1* OR^{His} lines, the callus cells from wild type control and the various transgenic lines were first digested using protoplast-releasing enzymes and observed under the light microscope. No orange objectives

were observed in Col-0 wild type control as well as in the *CmFBN1* only transgenic lines (Fig. 7A). While the OR^{His} line had a few relatively large circle-shaped orange objectives as large chromoplasts as shown previously (Sun et al. 2020b), the *CmFBN1* OR^{His} lines produced many smaller dot orange structures (Fig. 7A), showing alteration of the carotenoid accumulating structures when *CmFBN1* was coexpressed with OR^{His}.

To examine whether *CmFBN1* promoted plastoglobule proliferation for carotenoid accumulation in the *CmFBN1* OR^{His} lines, plastid ultrastructures in the callus cells of Col-0, *CmFBN1*, OR^{His}, and *CmFBN1* OR^{His} lines were analyzed by transmission electron microscopy (TEM). As shown in Fig. 7B, plastids or leucoplasts were observed in the callus cells of Col-0. When *CmFBN1* was expressed by itself, there was no great difference in plastid morphology in the callus cells from *CmFBN1* and Col-0. The OR^{His} callus cells had plastids with membrane structures, consistent with previous observations of membranous chromoplasts (Yuan et al. 2015a). However, the *CmFBN1* OR^{His} callus cells harbored morphologically different plastids from the OR^{His} calli. Plastids from *CmFBN1* OR^{His} samples clearly contained many plastoglobules with high electron density (Fig. 7B).

We next counted the number of plastoglobules in the plastids from the callus cells of Col-0, *CmFBN1*, OR^{His}, and *CmFBN1* OR^{His}. Col-0 had an average of 0.83 plastoglobules per plastid. *CmFBN1* and OR^{His} contained an average of 0.33 and 0.67 plastoglobules per plastid, respectively. In contrast, the *CmFBN1* OR^{His} samples contained an average of 12.75 plastoglobules per plastid (Fig. 7C), suggesting that *CmFBN1* facilitates plastoglobule proliferation. Notably, although OR^{His} calli contained similar numbers of plastoglobules as Col-0 and *CmFBN1* calli, OR^{His} calli harbored membrane chromoplasts for higher total carotenoid levels than Col-0 and *CmFBN1* calli with leucoplasts (Fig. 6). The expression of *CmFBN1* in the OR^{His} background changed the chromoplast type from membranous chromoplasts in the OR^{His} calli to globular chromoplasts in the *CmFBN1* OR^{His} samples (Fig. 7B).

CmFBN1 protein level is stabilized by OR

Although *CmFBN1* expressed higher in *low-β* than CEZ at mature stage, its protein level was lower in *low-β* (Fig. 4B and C), suggesting a requirement of CmOR for CmFBN1 protein stability. CmOR has been shown to stabilize PSY protein for carotenoid biosynthesis in melon fruit (Chayut et al. 2017). To examine whether CmOR was also able to stabilize CmFBN1 protein level in stimulating plastoglobule proliferation for carotenoid accumulation, we examined CmFBN1 protein level either in Col-0 or OR^{His} background by western blot analysis. As shown in Fig. 8A, much stronger protein bands of CmFBN1 were observed in the calli of the 3 *CmFBN1* OR^{His} lines than the 3 *CmFBN1* lines in Col-0 background. Relative quantification of the band intensity showed a significantly higher abundance of CmFBN1 protein for those *CmFBN1* OR^{His} lines than in the 3 *CmFBN1* lines (Fig. 8B). While 2 of the *CmFBN1* lines (#6 and #8) had lower *CmFBN1* expression, the #1 line exhibited comparable expression level as 2 of the *CmFBN1* OR^{His} lines (Fig. 6A). Thus, the high CmFBN1 protein levels in the *CmFBN1* OR^{His} lines were caused by the OR-enhanced CmFBN1 stability, not by high *CmFBN1* expression.

CmFBN1 protein accumulates in the plastoglobule-enriched fraction

To further investigate the role of CmFBN1 in stimulating OR^{His}-triggered carotenoid accumulation in plastoglobules, subplastidial fractionation by sucrose gradient ultracentrifugation was conducted with the callus samples from Col-0, *CmFBN1*, OR^{His}, and *CmFBN1* OR^{His} lines (Fig. 8C). Plastoglobules are lipoprotein particles, which are known to float on the top of the gradient (Nogueira et al. 2013; Morelli et al. 2022). Western blot analysis of CmFBN1-myc tagged proteins in the top plastoglobule fraction and the middle orange pigment containing fraction was carried out. A very low level of CmFBN1 proteins was detected in the top plastoglobule fraction of the callus samples from *CmFBN1* lines in Col-0 wild type background (Fig. 8D). In contrast, CmFBN1 proteins presented at high abundance in the top plastoglobule fraction from calli of *CmFBN1* OR^{His} (Fig. 8D), consistent with high total CmFBN1 protein levels in the *CmFBN1* OR^{His} lines in comparison with *CmFBN1* only transgenic lines (Fig. 8A). No CmFBN1 proteins were detected in the orange pigment containing the middle fraction of both samples (Fig. 8D). This data ascertains that CmFBN1 protein accumulates in the plastoglobules of OR^{His}-induced chromoplasts.

The carotenoid levels in these 2 fractions were also analyzed by ultraperformance convergence chromatography (UPC^2). The top plastoglobule fraction from calli of Col-0 and *CmFBN1* lines contained negligible amounts of carotenoids. The plastoglobule fraction from calli of OR^{His} had high level of total carotenoids, but was over 3-fold lower than that from calli of *CmFBN1* OR^{His} (Fig. 8E). Visible difference in carotenoid color can be clearly seen in the plastoglobule fraction of OR^{His} and of *CmFBN1* OR^{His} samples (Fig. 8C enlarged section). In the middle orange pigment containing fraction, the samples of OR^{His} also had lower total carotenoids than *CmFBN1* OR^{His}. The carotenoid compositions in calli of OR^{His} and *CmFBN1* OR^{His} as well as in the top and middle fractions were similar, although phytoene was detected in higher abundance in the top plastoglobule fraction from the calli of *CmFBN1* OR^{His} than the other samples. In melon fruit samples, plastoglobules are also more abundant in CEZ fruit compared to *low-β* fruit (Supplemental Fig. S12).

Discussion

Carotenoid accumulation in chromoplasts involves the formation of pigment lipoprotein sequestering substructures, which not only enable stable storage but also stimulate

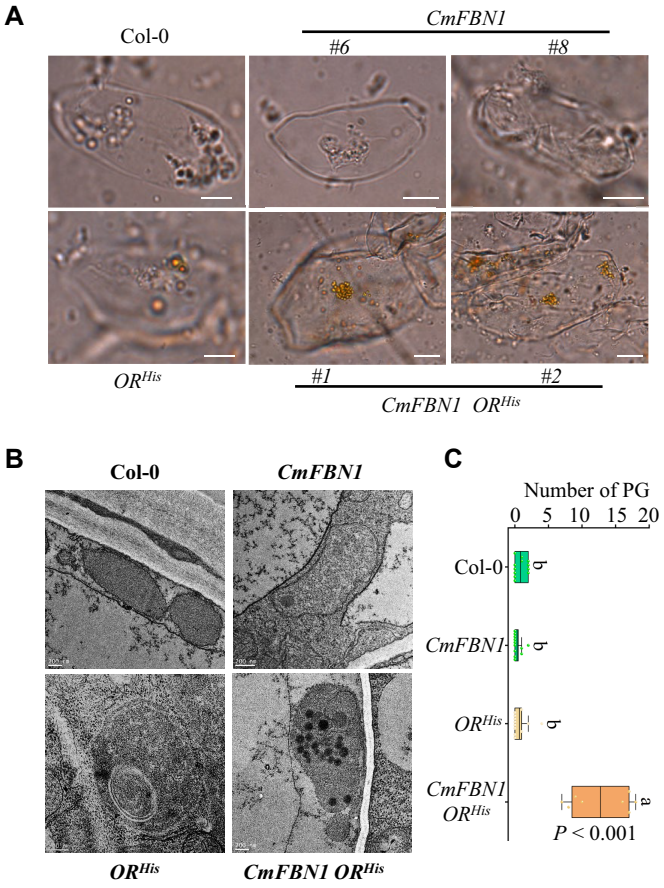

Figure 7. Microscopic analysis of callus cells from various lines. **A)** Phenotypes of protoplasts from calli of Col-0 wild type, *CmFBN1*, OR^{His}, and *CmFBN1* OR^{His} lines under light microscope. The formation of multiple small orange dot structures was observed in the *CmFBN1* OR^{His} lines but not in the OR^{His} line. Scale bar = 25 μm. **B)** Plastid ultrastructure of callus cells from various lines under TEM. High electron dense plastoglobules (PGs) are clearly seen in the sample of *CmFBN1* OR^{His}. Scale bar = 200 nm. **C)** Number of PG per plastid, counting from TEM images (n = 8 to 12). Box plots are used to show the distributions of data points. The lines in the box (from right to left) indicate the maximum, upper quartile, mean, lower quartile, and minimum. Different letters represent significant difference with $P < 0.001$, which was analyzed by Tukey's test.

biosynthesis (Li and Yuan 2013; Sun et al. 2018; Sun et al. 2022a). Plastoglobules are carotenoid sequestering substructures and are abundant in globular chromoplasts (Morelli et al. 2022). While FBN1 homologs are known to be localized in plastoglobules and to promote carotenoid accumulation, sound experimental data connecting these 2 observations with causality is missing. Melon orange flesh fruit contains globular chromoplasts (Jeffery et al. 2012). Here, we showed that CmFBN1 physically interacted with CmOR in plastoglobules. Such an interaction stabilizes CmFBN1 protein to stimulate plastoglobule proliferation and enhance OR-triggered carotenoid accumulation in chromoplasts.

Proteome profiling identifies CmFBN1 involved in CmOR-regulated carotenoid accumulation in chromoplasts

CmOR acquired a specific function to induce chromoplast formation for high levels of β-carotene accumulation, giving melon fruit an orange flesh color (Tzuri et al. 2015; Chayut et al. 2017). CmOR represents a *bona fide* molecular switch of chromoplast formation for carotenoid accumulation. Melon varieties CEZ and *low-β* are isogenic lines with CEZ containing functional CmOR to promote chromoplast biogenesis and *low-β* having a truncated, malfunctional CmOR with impaired chromoplast formation (Chayut et al. 2017). Thus, they provide excellent genetic resources to identify genes and proteins associated with the CmOR-controlled chromoplast development and carotenoid accumulation. By using comparative proteomic analysis, we identified CmFBN1 among the top differentially expressed proteins in the mature fruit.

FBN1 is the most abundant protein involved in carotenoid sequestration and accumulation in fibrillar chromoplasts of pepper fruit and cucumber flowers (Vishnevetsky et al. 1996; Pozueta-Romero et al. 1997; Wang et al. 2013). FBN homologs are also found in other kinds of chromoplasts from other fruits and flowers as well as in other types of plastids in plant tissues (Singh and McNellis 2011; Kim and Kim 2022). Among 9 members of the *CmFBN* gene family,

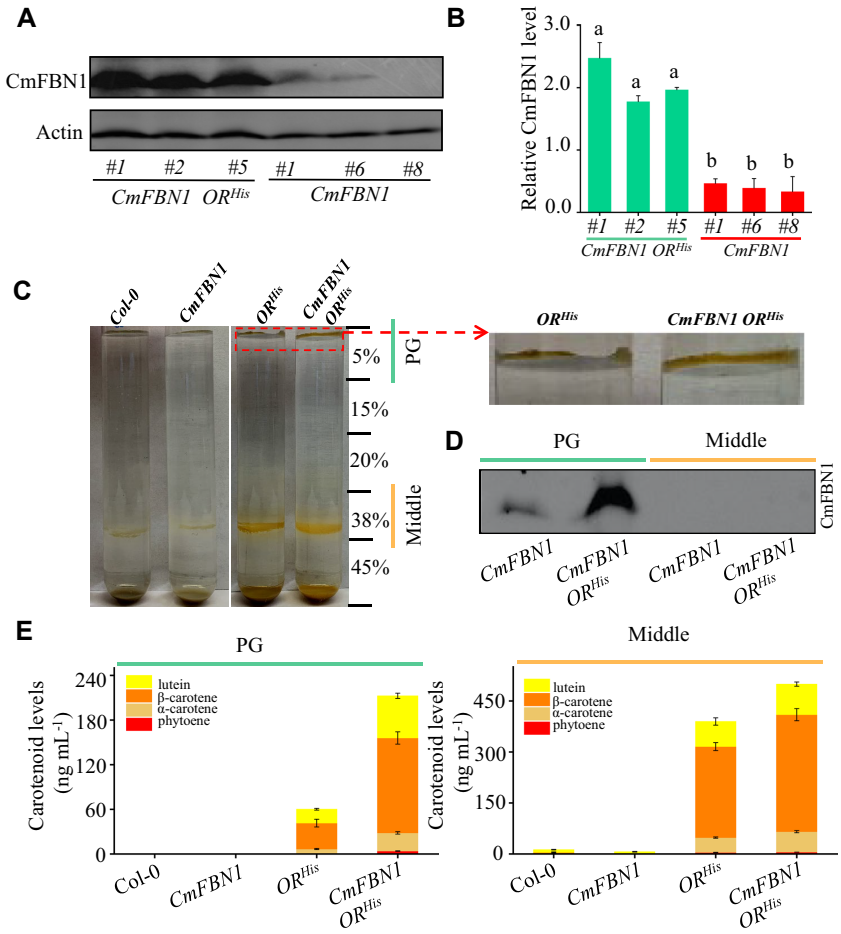

Figure 8. Analysis of total CmFBN1 protein level and subplastidal fractionation of CmFBN1 from callus samples of *CmFBN1 OR^{His}* and *CmFBN1* transgenic lines. **A)** Western blot analysis of CmFBN1 protein levels in calli of various lines. Actin bands show protein loading. **B)** Relative CmFBN1 protein levels were determined by measuring the band density of western blot images using ImageJ software and normalizing to actin from 3 independent biological replicates. Data are means ± SD of 3 biological replicates, which was analyzed by Tukey's test ($P < 0.05$). **C)** Sucrose gradient fractionation of the subchromoplast components from calli of various lines. The top box shows the plastoglobule (PG) fraction including enlarged section. **D)** Western blot analysis of CmFBN1 protein levels in the PG and orange pigment containing middle (Middle) fractions of C from *CmFBN1* and *CmFBN1 OR^{His}* transgenic lines. **E)** Carotenoid levels of PG and Middle fractions of **C**) from calli of various lines. Data are means ± SD of 3 biological replicates, which was analyzed by Tukey's test ($P < 0.05$).

CmFBN1 is the only gene expressed highly in fruit tissue, suggesting its specific role in carotenoid accumulation in melon fruit. CmFBN1 protein level was lower in *low-β* than CEZ at mature stage (Fig. 4C), while its gene expression was higher in *low-β* fruit (Fig. 4B). The high gene expression but low protein level suggests reduced stability of CmFBN1 protein in the absence of functional CmOR in *low-β*.

CmFBN1 physically interacts with CmOR to enhance its protein stability and exert its function

OR serves as a multifunctional protein for plastid development and carotenoid accumulation (Sun et al. 2022a). OR was found to directly interact with and stabilize a few plastidial proteins in plants (Chayut et al. 2017; Kang et al. 2017; Yuan et al. 2021; Sun et al. 2023). In addition, OR^{His} interferes with the association of plastid division proteins to regulate chromoplast division (Sun et al. 2020b). CmOR interacts with and stabilizes CmPSY1, and loss of CmOR function results in very low levels of PSY and carotenoid accumulation in *low-β* (Chayut et al. 2017). Interestingly, we found here that CmFBN1 also physically interacted with CmOR (Fig. 5). Furthermore, the CmFBN1 protein level was much higher in the *OR^{His}* background than in the control (Fig. 8A), showing the role of OR in stabilizing CmFBN1 and consisting with its chaperone function in enhancing its interacting protein stability.

FBNs were reported to interact with several proteins and their interaction partners define their functions (Singh and McNellis 2011; Kim and Kim 2022). AtFBN1a and AtFBN1b interact with starch synthase 4 to initiate starch granule formation at the specific region of the thylakoid membrane adjacent to plastoglobules in Arabidopsis (Gamez-Arjona et al. 2014). AtFBN5 physically associates with solanesyl diphosphate

synthase 1 and 2 for the synthesis of the lipid tail of plastoquinone-9 in chloroplasts (Kim et al. 2015). AtFBN1/2 binds to allene oxide synthase to mediate jasmonate-modulated anthocyanin accumulation (Torres-Romero et al. 2022). The direct interaction of CmFBN1 with CmOR positions its function in association with the CmOR-regulated chromoplast development and carotenoid accumulation in melon fruit.

CmFBN1 functions in the CmOR-regulated chromoplast development and carotenoid accumulation

CmOr and its genetic mimic OR^{His} are known to regulate chromoplast formation (Tzuri et al. 2015; Yuan et al. 2015a; Chayut et al. 2017; Yazdani et al. 2019). Previously, we have established an Arabidopsis callus system with chromoplast development program by expression of OR^{His} to investigate genes/proteins that are involved with chromoplast development and carotenoid accumulation (Yuan et al. 2015a). By using this system, we have defined the functional roles of plastid division factors on chromoplast division and carotenoid accumulation (Sun et al. 2020b).

CmFBN1 overexpression in the wild type Col-0 background showed minimal effect on carotenoid accumulation. However, when *CmFBN1* was expressed in the Arabidopsis OR^{His} line, it significantly enhanced carotenoid levels in the calli (Fig. 6), a tissue where carotenoid accumulation is positively associated with the factors affecting this process (Bai et al. 2014; Schaub et al. 2018). These results support the function of CmFBN1 in the CmOR-regulated carotenoid accumulation in chromoplasts.

Overexpression of a pepper *FBN1* causes a 2-fold increase of carotenoid content in tomato fruit under a chromoplast development program (Simkin et al. 2007). Suppression of tomato *FBN1* expression by RNAi results in 30% reduction of carotenoids in transgenic tomato flowers (Leitner-Dagan et al. 2006). In tomato *high-pigment1* fruit at red ripe stage, *FBN* expression is increased and believed to contribute to the enhanced carotenoid content by sequestrating and stabilizing carotenoids in chromoplasts (Kilambi et al. 2013). Similarly, FBN protein levels increase with enhanced carotenoid accumulation when leaf chloroplasts were artificially differentiated into leaf chromoplasts (Llorente et al. 2020; Morelli et al. 2022). Our study along with these reports substantiates the role of FBNs in carotenoid accumulation in chromoplasts.

CmFBN1 promotes carotenoid accumulation via stimulating plastoglobule proliferation in chromoplasts

FBNs are involved in the formation of plastid lipoprotein structures and represent abundant proteins in plastoglobules (Singh and McNellis 2011; Kim and Kim 2022). Plastoglobules are abundant in globular chromoplasts to sequester and store carotenoids (Nogueira et al. 2013; Morelli et al. 2022). When CmFBN1-cYFP and CmOR-nYFP interacted, the interaction signals were localized in plastoglobules (Fig. 5). Interestingly, while OR^{His} by itself induced the formation of membranous chromoplasts in the callus cells (Yuan et al. 2015a), *CmFBN1* altered the plastid ultrastructure in the OR^{His} background. Many plastoglobules with high electron density as shown in other studies (Nogueira et al. 2013; Morelli et al. 2022) were clearly observed in the callus cells of the *CmFBN1* OR^{His} lines in comparison with the OR^{His} lines (Fig. 7), showing that CmFBN1 facilitated plastoglobule proliferation. Moreover, CmFBN1 protein presented abundantly in the plastoglobule-enriched fraction following sucrose gradient ultracentrifugation of plastids from callus cells of the *CmFBN1* OR^{His} lines (Fig. 8). This further documents the role of OR in promoting CmFBN1 accumulation and confirms CmFBN1 function in promoting plastoglobule proliferation in chromoplasts. The observed plastoglobule proliferation in the plastids of *CmFBN1* OR^{His} callus cells was also found in the crtB-induced leaf chromoplasts, where FBN1 protein levels are enhanced (Llorente et al. 2020; Morelli et al. 2022).

Plastoglobules are known to be the site for carotenoid sequestration and accumulation in globular chromoplasts. Melon fruit contains globular chromoplasts (Jeffery et al. 2012), which are characterized by abundant plastoglobules (Sun et al. 2018; Hermanns et al. 2020). Thus, CmFBN1 likely plays an important role in the CmOR-induced chromoplast development and β-carotene accumulation in melon fruit. The model of CmFBN1 participating in carotenoid accumulation in chromoplasts is shown in Fig. 9. The demonstration of *CmFBN1* in promoting carotenoid accumulation in a cell with chromoplast development program suggests the potential of *FBN1* gene to serve as a genetic target in association with chromoplast development for carotenoid enrichment in crops.

Materials and methods

Melon plant materials

The melon (*C. melo*) varieties used in this study were CEZ with orange fleshed fruit and the *low-β* mutant, an EMS-mutated CEZ isogenic line with light green fleshed fruit (Chayut et al. 2017; Chayut et al. 2021). They were grown either in the field or in a greenhouse with a 14-h light and 10-h dark. Four fruits from 4 plants of each genotype were harvested at mature stage. The root, stem, leaf, flower, and flesh tissues were frozen immediately and stored at −80 °C until use.

Metabolite determination

Total carotenoids from frozen samples (0.2 g) were extracted according to the method as described (Cao et al. 2019). The extracted pigments were analyzed using UPC^2 as detailed previously (Yazdani et al. 2019; Sun et al. 2021). Quantification was performed using commercial β-carotene as the calibration standard. Tocopherols and ubiquinone-10 from 4-week-old Arabidopsis (*A. thaliana*) calli (100 mg) were extracted in 1 mL of hexane: methanol:

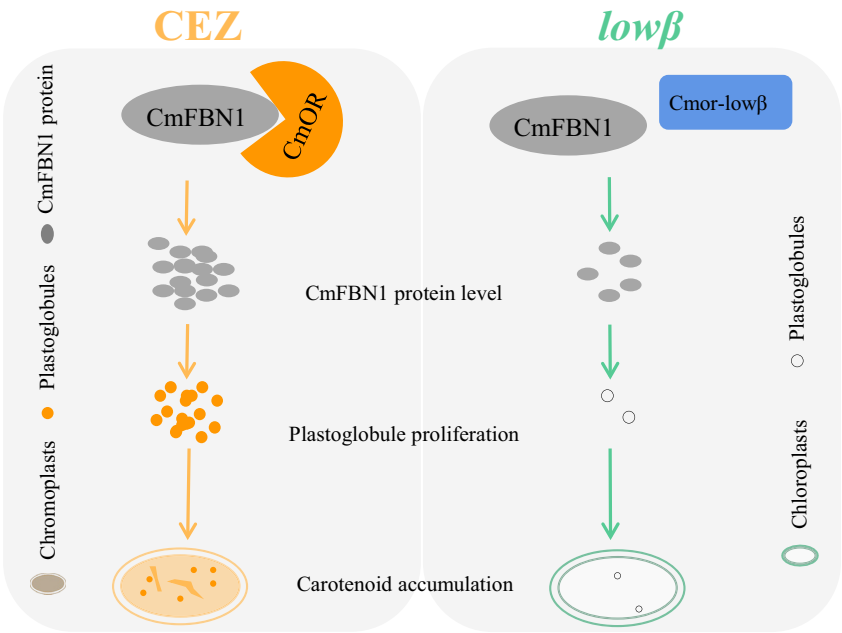

Figure 9. Model of CmFBN1 in the CmOR-regulated β-carotene accumulation in melon fruit. In CEZ orange variety, CmFBN1 physically interacts with CmOR, which stabilizes CmFBN1 protein. The enhanced CmFBN1 protein level stimulates plastoglobule proliferation in chromoplasts to facilitate the CmOR-regulated carotenoid accumulation to give orange flesh fruit. In *low-β* mutant, the lack of functional CmOR impairs its interaction with CmFBN1, resulting in low stability of CmFBN1 and plastoglobule proliferation with low level of β-carotene accumulation.

acetone (2:1:1; v/v/v). The metabolites were separated on a C18 column (Acquity BEH Shield RP18 1.7 μm 2.1 × 100 mm) using an Acquity UPLC system (Waters, USA). Identification and quantification of metabolites were achieved by comparing the retention time and absorption spectra with authentic standards and by using external standard calibration curves.

Proteomic analysis

Total proteins from fruit of CEZ and *low-β* mutant at mature stage with 3 biological replicates were extracted as described previously (Yang et al. 2007). Proteins (50 μg) from each sample were digested, labeled using Tandem Mass Tag (TMT) 10-plex reagents, fractionated, and subjected to mass spectrometer analysis. The mass spectrometry proteomics data were deposited to the ProteomeXchange Consortium via the PRIDE partner repository with the dataset identifier PXD033294 and 10.6019/PXD033294. The detailed method for the proteomic analysis can be found in Methods S1.

Gene expression analysis

Total RNA extraction and RT-qPCR analysis were performed as detailed previously (Chayut et al. 2021). For digital expression of *CmFBN* genes, RPKM values were obtained from online melon RNA-Seq data (http://cucurbitgenomics.org/organism/18).

Subcellular localization

CmFBN1, *CmOr*, and *Cmor-lowβ* without stop codons were amplified using gene-specific primers (Supplemental Table S1) and cloned into pGWB541 vector to produce YFP fusion protein constructs. *AtFBN4* as a plastoglobule marker was cloned into pPZP-Bar-mCherry vector to produce AtFBN4-mCherry fusion protein construct. The *CmFBN1*, *CmOr*, and *Cmor-lowβ* constructs were infiltrated individually or coinfiltrated with *AtFBN4-mCherry* construct into 4-week-old *N. benthamiana* leaves. Three days after infiltration, the infiltrated leaves were examined under Leica TCS SP5 Laser Scanning Confocal Microscope (Leica Microsystems, Exton, PA, USA) as detailed (Sun et al. 2020a). For the detection of the YFP and chlorophyll fluorescence, excitation light wavelength was set at 488 nm and emission filter was at 520 to 560 nm for YFP and at 620 to 680 nm for chlorophyll.

Y2H analysis

Y2H analysis was carried out utilizing the split ubiquitin system as detailed (Sun et al. 2022b). *CmFBN1*, *CmOr*, and *Cmor-lowβ* without the transit peptide coding sequences and stop codons were amplified using gene-specific primers (Supplemental Table S1) and inserted separately into the pMetYc vector to produce *CmOr-Cub* and *Cmor-lowβ-Cub* plasmids and into pNX33 vector to generate *CmFBN1-Nub* plasmid. The paired Nub and Cub plasmids were cotransformed into yeast (*Saccharomyces cerevisiae*) strain THY.AP4 and plated out with 5- to 10-fold dilutions on either nonselection DDO (-Leu/-Trp) or selection TDO (-Leu/-Trp/-His) medium with 1 mM 3-AT. To quantify the interaction strength, the β-galactosidase activity assay was performed as detailed (Yuan et al. 2021).

Bimolecular fluorescence complementation (BiFC)

Melon *CmFBN1* and *Cmor-lowβ* CDS without stop codons were amplified from CEZ and *low-β* fruit cDNA, respectively, using gene specific primers (Supplemental Table S1) and ligated into pDONR207 vector. They were subcloned into pSITE-cEYFP-N1 vector to produce *CmFBN1-cEYFP* and *Cmor-lowβ-nEYFP* constructs. The *CmOR-nYFP* plasmid was generated previously (Chayut et al. 2021). A pair of BiFC constructs along with controls or *AtFBN4-mCherry* construct was coinfiltrated into 4-week-old *N. benthamiana* leaves and the fluorescence images were captured as described (Sun et al. 2022b). For the detection of the YFP and chlorophyll fluorescence, excitation light wavelength was set at 488 nm and emission filter was at 520 to 560 nm for YFP and at 620 to 680 nm for chlorophyll.

Generation of transgenic *CmFBN1* lines in Arabidopsis and seed-derived callus induction

To generate *CmFBN1* transgenic overexpression lines in Arabidopsis, *CmFBN1* CDS without stop codon was amplified from CEZ melon fruit using primers (Supplemental Table S1) and cloned into the binary vector pGWB17. The construct was transformed into Arabidopsis wild type (Col-0) and the OR^{His} overexpression transgenic plants generated previously (Yuan et al. 2015a). Western blot analysis with anti-Myc antibody (Sigma-Aldrich) was used to identify *CmFBN1* overexpression transgenic lines. The Arabidopsis seed-derived calli were induced following the protocol as described (Yuan et al. 2015a).

Western blot analysis

Total proteins from leaf and callus tissue of Col-0 and transgenic lines were extracted and used for western blot analysis following the methods as described (Sun et al. 2020b). Proteins (30 μg) were separated on 12% (v/v) sodium dodecyl-sulfate polyacrylamide gel electrophoresis (SDS-PAGE) gel, probed, and detected using a WesternBright ECL kit (LPS Cat# K-12045-D20). For loading control, the membrane was stripped using a stripping buffer (Welsch et al. 2018) and reprobed with anti-Actin antibody (Sigma). The western blot bands from 3 biological replicate membranes were quantified using ImageJ software.

Microscopy analysis

For light microscopic observation, protoplasts from calli were isolated following the method as previously described (Sun et al. 2020b). In brief, 4-week-old calli were digested in an enzyme solution for 6 h in darkness with gentle shaking. The digested samples were loaded onto well slides and observed under a bright field using a DM5500 microscope (Leica).

For TEM analysis, Arabidopsis calli of Col-0, *CmFBN1*, OR^{His}, and *CmFBN1* OR^{His} were collected, fixed, embedded, and sectioned following the protocol as described (Sun et al. 2019). The resulting sections were viewed under a transmission electron microscope at Cornell Center for Materials Research (https://www.ccmr.cornell.edu/transmission-electron-microscopy/).

Subplastidial fractionation by sucrose gradient ultracentrifugation

Subplastidial fractionation by sucrose gradient ultracentrifugation was performed as reported (Nogueira et al. 2013). Briefly, 4-week-old calli (10 g) from Col-0, *CmFBN1*, OR^{His}, and *CmFBN1* OR^{His} lines were ground in the extraction buffer (0.4 M sucrose, 50 mM Tris, pH 7.8, 1 mM EDTA, and 1 mM DTT). The homogenates were filtered and centrifuged at 5,000 g for 10 min. Pellets were resuspended in 3 mL of 45% (w/v) sucrose buffer, manually homogenized, and overlaid with a discontinuous sucrose gradient consisting of 2 mL of 38% (w/v), 2 mL of 20% (w/v), 2 mL of 15% (w/v), and 2 mL of 5% (w/v) sucrose buffer. The samples were centrifuged at 28,000 g for 8 h at 4 °C. The top fraction (2 mL) and the middle orange color fraction (2 mL) were collected and used for carotenoid analysis by UPC[2] and western blot analysis after extraction of proteins according to Nogueira et al. (2013).

Bioinformatics analysis

All statistical analyses were undertaken using Microsoft Excel software. For selection of proteins with different abundances between CEZ and *low-β* mutant fruit, the criteria of fold change > 1.5 or < 0.67 (P-value < 0.05) cut-off were used.

Phylogenetic trees were constructed using Molecular Evolutionary Genetics Analysis version 5.0 software with 1,000 bootstrap replicates and neighbor-joining methods. The full-length protein sequences were aligned using Clustal X 2.1 software (Larkin et al. 2007). Heatmap was generated using software OriginPro 2021 (https://www.originlab.com/). Protein pathway analysis was carried out using KEGG (http://www.genome.jp/kegg/). Volcano plot and PC analysis were prepared using OriginPro 2021 (https://www.originlab.com/).

Accession numbers

Sequence data from this article can be found in the GenBank/EMBL data libraries under accession numbers CmFBN1 (XP_008440050) and CmOR (XP_008467325).

Acknowledgments

We thank John Grazul for aiding the TEM analysis. The authors acknowledge the use of facilities and instrumentation supported by NSF through the Cornell University Materials Research Science and Engineering Center DMR-1719875. X.Z. acknowledges the graduate training scholarship from the China Scholarship Council (CSC).

Author contributions

X.Z. and L.L. planned and designed the research. X.Z. performed most of the experiments. T.S., L.O., E.W., and A.L. aided some experiments. Y.Y. and T.F. performed proteomic analysis. T.F. aided carotenoid analysis. H.Y. extracted

proteins for proteomic analysis. N.C., J.B., and Y.T. grew melon plants in the field. Y.T., T.T., W.G., and L.C. assisted data analysis and critically edited the manuscript. WG and L.L. supervised, and X.Z. and L.L. wrote the article with contributions from all coauthors.

Supplemental data

The following materials are available in the online version of this article.

Supplemental Figure S1. Schematic carotenoid biosynthesis pathway in plants.

Supplemental Figure S2. Carotenoid levels in CEZ and *low-β* and plant growth phenotype.

Supplemental Figure S3. The alignment and transmembrane domain analysis of CmOR and Cmor-lowβ.

Supplemental Figure S4. Kyoto Encyclopedia of Genes and Genomes (KEGG) pathway analysis.

Supplemental Figure S5. Photosynthesis, photosynthesis-antenna proteins, and carbon fixation in photosynthetic organisms.

Supplemental Figure S6. A heatmap of expression of carotenoid biosynthesis pathway genes at different melon fruit developmental stages.

Supplemental Figure S7. The negative controls of BiFC assay.

Supplemental Figure S8. Interaction of CmFBN2 and CmFBN3 with CmOR and negative controls in BiFC assay.

Supplemental Figure S9. Lutein level in callus tissue of various lines.

Supplemental Figure S10. qPCR analysis of expression of endogenous carotenoid metabolic genes in various lines.

Supplemental Figure S11. Tocopherol and ubiquinone-10 levels in callus tissue of various lines.

Supplemental Figure S12. Sucrose gradient fractionation of the subchromoplast components from CEZ and *low-β*.

Supplemental Table S1. List of primers used in this study.

Supplemental Methods S1. Detail method of proteomic analysis.

Supplemental Data Set 1. Differently expressed proteins in *low-β* compared to CEZ at the mature stage.

Supplemental Data Set 2. GO functional analysis of the differentially expressed proteins in *low-β* compared to CEZ at the mature stage.

Supplemental Data Set 3. KEGG pathway analysis of the differentially expressed proteins in *low-β* compared to CEZ at the mature stage.

Funding

This work was supported by Agriculture and Food Research Initiative competitive awards grant no. 2019-67013-29162 from the United States Department of Agriculture National Institute of Food and Agriculture and the USDA-ARS fund.

Conflict of interest statement. None declared.

Data availability

The data that support the findings of this study are available from the corresponding authors upon request.

References

Al-Babili S, Bouwmeester HJ. Strigolactones, a novel carotenoid-derived plant hormone. Annu Rev Plant Biol. 2015:**66**(1):161–186. https://doi.org/10.1146/annurev-arplant-043014-114759

Alvarez D, Voss B, Maass D, Wust F, Schaub P, Beyer P, Welsch R. Carotenogenesis is regulated by 5'UTR-mediated translation of phytoene synthase splice variants. Plant Physiol. 2016:**172**(4):2314–2326. https://doi.org/10.1104/pp.16.01262

Auldridge ME, McCarty DR, Klee HJ. Plant carotenoid cleavage oxygenases and their apocarotenoid products. Curr Opin Plant Biol. 2006:**9**(3):315–321. https://doi.org/10.1016/j.pbi.2006.03.005

Bai C, Rivera SM, Medina V, Alves R, Vilaprinyo E, Sorribas A, Canela R, Capell T, Sandmann G, Christou P, et al. An in vitro system for the rapid functional characterization of genes involved in carotenoid biosynthesis and accumulation. Plant J. 2014:**77**(3):464–475. https://doi.org/10.1111/tpj.12384

Beltran JC, Stange C. Apocarotenoids: a new carotenoid-derived pathway. Subcell Biochem. 2016:**79**:239–272. https://doi.org/10.1007/978-3-319-39126-7_9

Cao H, Luo H, Yuan H, Eissa MA, Thannhauser TW, Welsch R, Hao YJ, Cheng L, Li L. A neighboring aromatic-aromatic amino acid combination governs activity divergence between tomato phytoene synthases. Plant Physiol. 2019:**180**(4):1988–2003. https://doi.org/10.1104/pp.19.00384

Cazzonelli CI, Pogson BJ. Source to sink: regulation of carotenoid biosynthesis in plants. Trends Plant Sci. 2010:**15**(5):266–274. https://doi.org/10.1016/j.tplants.2010.02.003

Chayut N, Yuan H, Ohali S, Meir A, Sa'ar U, Tzuri G, Zheng Y, Mazourek M, Gepstein S, et al. Distinct mechanisms of the ORANGE protein in controlling carotenoid flux. Plant Physiol. 2017:**173**(1):376–389. https://doi.org/10.1104/pp.16.01256

Chayut N, Yuan H, Ohali S, Meir A, Yeselson Y, Portnoy V, Zheng Y, Fei Z, Lewinsohn E, Katzir N, et al. A bulk segregant transcriptome analysis reveals metabolic and cellular processes associated with orange allelic variation and fruit β-carotene accumulation in melon fruit. BMC Plant Biol. 2015:**15**(1):274. https://doi.org/10.1186/s12870-015-0661-8

Chayut N, Yuan H, Saar Y, Zheng Y, Sun T, Zhou X, Hermanns A, Oren E, Faigenboim A, Hui M, et al. Comparative transcriptome analyses shed light on carotenoid production and plastid development in melon fruit. Hortic Res. 2021:**8**(1):112. https://doi.org/10.1038/s41438-021-00547-6

D'Alessandro S, Havaux M. Sensing β-carotene oxidation in photosystem II to master plant stress tolerance. New Phytol. 2019:**223**(4):1776–1783. https://doi.org/10.1111/nph.15924

Deruere J, Romer S, d'Harlingue A, Backhaus RA, Kuntz M, Camara B. Fibril assembly and carotenoid overaccumulation in chromoplasts: a model for supramolecular lipoprotein structures. Plant Cell. 1994:**6**(1): 119–133. https://doi.org/10.1105/tpc.6.1.119

Domonkos I, Kis M, Gombos Z, Ughy B. Carotenoids, versatile components of oxygenic photosynthesis. Prog Lipid Res. 2013:**52**(4):539–561. https://doi.org/10.1016/j.plipres.2013.07.001

Egea I, Barsan C, Bian W, Purgatto E, Latche A, Chervin C, Bouzayen M, Pech JC. Chromoplast differentiation: current status and perspectives. Plant Cell Physiol. 2010:**51**(10):1601–1611. https://doi.org/10.1093/pcp/pcq136

Fiedor J, Burda K. Potential role of carotenoids as antioxidants in human health and disease. Nutrients. 2014:**6**(2):466–488. https://doi.org/10.3390/nu6020466

Fraser PD, Bramley PM. The biosynthesis and nutritional uses of carotenoids. Prog Lipid Res. 2004:**43**(3):228–265. https://doi.org/10.1016/j.plipres.2003.10.002

Galpaz N, Wang Q, Menda N, Zamir D, Hirschberg J. Abscisic acid deficiency in the tomato mutant *high-pigment 3* leading to increased plastid number and higher fruit lycopene content. Plant J. 2008:**53**(5):717–730. https://doi.org/10.1111/j.1365-313X.2007.03362.x

Gamez-Arjona FM, Raynaud S, Ragel P, Merida A. Starch synthase 4 is located in the thylakoid membrane and interacts with plastoglobule-associated proteins in Arabidopsis. Plant J. 2014:**80**(2):305–316. https://doi.org/10.1111/tpj.12633

Havaux M. β-cyclocitral and derivatives: emerging molecular signals serving multiple biological functions. Plant Physiol Biochem. 2020:**155**:35–41. https://doi.org/10.1016/j.plaphy.2020.07.032

Hermanns AS, Zhou X, Xu Q, Tadmor Y, Li L. Carotenoid pigment accumulation in horticultural plants. Hortic Plant J. 2020:**6**(6):343–360. https://doi.org/10.1016/j.hpj.2020.10.002

Jeffery J, Holzenburg A, King S. Physical barriers to carotenoid bioaccessibility. Ultrastructure survey of chromoplast and cell wall morphology in nine carotenoid-containing fruits and vegetables. J Sci Food Agric. 2012:**92**(13):2594–2602. https://doi.org/10.1002/jsfa.5767

Kachanovsky DE, Filler S, Isaacson T, Hirschberg J. Epistasis in tomato color mutations involves regulation of *phytoene synthase 1* expression by cis-carotenoids. Proc Natl Acad Sci U S A. 2012:**109**(46):19021–19026. https://doi.org/10.1073/pnas.1214808109

Kall L, Krogh A, Sonnhammer EL. Advantages of combined transmembrane topology and signal peptide prediction–the phobius web server. Nucleic Acids Res. 2007:**35**(Web Server):W429–W432. https://doi.org/10.1093/nar/gkm256

Kang L, Kim HS, Kwon YS, Ke Q, Ji CY, Park SC, Lee HS, Deng X, Kwak SS. Ibor regulates photosynthesis under heat stress by stabilizing IbPsbP in sweetpotato. Front Plant Sci. 2017:**8**:989. https://doi.org/10.3389/fpls.2017.00989

Kilambi HV, Kumar R, Sharma R, Sreelakshmi Y. Chromoplast-specific carotenoid-associated protein appears to be important for enhanced accumulation of carotenoids in *hp1* tomato fruits. Plant Physiol. 2013:**161**(4):2085–2101. https://doi.org/10.1104/pp.112.212191

Kim I, Kim HU. The mysterious role of fibrillin in plastid metabolism: current advances in understanding. J Exp Bot. 2022;**73**(9):2751–2764. https://doi.org/10.1093/jxb/erac087

Kim EH, Lee Y, Kim HU. Fibrillin 5 is essential for plastoquinone-9 biosynthesis by binding to solanesyl diphosphate synthases in Arabidopsis. Plant Cell. 2015:**27**(10):2956–2971. https://doi.org/10.1105/tpc.15.00707

Kolotilin I, Koltai H, Tadmor Y, Bar-Or C, Reuveni M, Meir A, Nahon S, Shlomo H, Chen L, Levin I. Transcriptional profiling of *high pigment*-2^{dg} tomato mutant links early fruit plastid biogenesis with its overproduction of phytonutrients. Plant Physiol. 2007:**145**(2):389–401. https://doi.org/10.1104/pp.107.102962

Larkin MA, Blackshields G, Brown NP, Chenna R, McGettigan PA, McWilliam H, Valentin F, Wallace IM, Wilm A, Lopez R, et al. Clustal W and clustal X version 2.0. Bioinformatics. 2007:**23**(21):2947–2948. https://doi.org/10.1093/bioinformatics/btm404

Leitner-Dagan Y, Ovadis M, Shklarman E, Elad Y, Rav David D, Vainstein A. Expression and functional analyses of the plastid lipid-associated protein CHRC suggest its role in chromoplastogenesis and stress. Plant Physiol. 2006:**142**(1):233–244. https://doi.org/10.1104/pp.106.082404

Li L, Lu S, O'Halloran DM, Garvin DF, Vrebalov J. High-resolution genetic and physical mapping of the cauliflower high-β-carotene gene *Or* (*Orange*). Mol Genet Genomics. 2003:**270**(2):132–138. https://doi.org/10.1007/s00438-003-0904-5

Li L, Yuan H. Chromoplast biogenesis and carotenoid accumulation. Arch Biochem Biophys. 2013:**539**(2):102–109. https://doi.org/10.1016/j.abb.2013.07.002

Liu Z, Yan H, Wang K, Kuang T, Zhang J, Gui L, An X, Chang W. Crystal structure of spinach major light-harvesting complex at 2.72 A resolution. Nature. 2004:**428**(6980):287–292. https://doi.org/10.1038/nature02373

Llorente B, Torres-Montilla S, Morelli L, Florez-Sarasa I, Matus JT, Ezquerro M, D'Andrea L, Houhou F, Majer E, Pico B, et al. Synthetic conversion of leaf chloroplasts into carotenoid-rich plastids reveals mechanistic basis of natural chromoplast development. Proc Natl Acad Sci U S A. 2020:**117**(35):21796–21803. https://doi.org/10.1073/pnas.2004405117

Lu S, Van Eck J, Zhou X, Lopez AB, O'Halloran DM, Cosman KM, Conlin BJ, Paolillo DJ, Garvin DF, Vrebalov J, et al. The cauliflower *Or* gene encodes a DnaJ cysteine-rich domain-containing protein that mediates high levels of beta-carotene accumulation. Plant Cell. 2006:**18**(12):3594–3605. https://doi.org/10.1105/tpc.106.046417

Maass D, Arango J, Wust F, Beyer P, Welsch R. Carotenoid crystal formation in Arabidopsis and carrot roots caused by increased phytoene synthase protein levels. PLoS One. 2009:**4**(7):e6373. https://doi.org/10.1371/journal.pone.0006373

Martel C, Vrebalov J, Tafelmeyer P, Giovannoni JJ. The tomato MADS-box transcription factor RIPENING INHIBITOR interacts with promoters involved in numerous ripening processes in a COLORLESS NONRIPENING-dependent manner. Plant Physiol. 2011:**157**(3):1568–1579. https://doi.org/10.1104/pp.111.181107

Moise AR, Al-Babili S, Wurtzel ET. Mechanistic aspects of carotenoid biosynthesis. Chem Rev. 2014:**114**(1):164–193. https://doi.org/10.1021/cr400106y

Morelli L, Torres-Montilla S, Glauser G, Shanmugabalaji V, Kessler F, Rodriguez-Concepcion M. Novel insights into the contribution of plastoglobules and reactive oxygen species to chromoplast differentiation. New Phytol. 2022;**237**(5):1696–1710. https://doi.org/10.1111/nph.18585

Moreno JC, Mi J, Alagoz Y, Al-Babili S. Plant apocarotenoids: from retrograde signaling to interspecific communication. Plant J. 2021:**105**(2):351–375. https://doi.org/10.1111/tpj.15102

Newman LA, Hadjeb N, Price CA. Synthesis of two chromoplast-specific proteins during fruit development in *Capsicum annuum*. Plant Physiol. 1989:**91**(2):455–458. https://doi.org/10.1104/pp.91.2.455

Nisar N, Li L, Lu S, Khin NC, Pogson BJ. Carotenoid metabolism in plants. Mol Plant. 2015:**8**(1):68–82. https://doi.org/10.1016/j.molp.2014.12.007

Niyogi KK, Truong TB. Evolution of flexible non-photochemical quenching mechanisms that regulate light harvesting in oxygenic photosynthesis. Curr Opin Plant Biol. 2013:**16**(3):307–314. https://doi.org/10.1016/j.pbi.2013.03.011

Nogueira M, Mora L, Enfissi EM, Bramley PM, Fraser PD. Subchromoplast sequestration of carotenoids affects regulatory mechanisms in tomato lines expressing different carotenoid gene combinations. Plant Cell. 2013:**25**(11):4560–4579. https://doi.org/10.1105/tpc.113.116210

Park S, Kim HS, Jung YJ, Kim SH, Ji CY, Wang Z, Jeong JC, Lee HS, Lee SY, Kwak SS. Orange protein has a role in phytoene synthase stabilization in sweetpotato. Sci Rep. 2016:**6**(1):33563. https://doi.org/10.1038/srep33563

Pozueta-Romero J, Rafia F, Houlne G, Cheniclet C, Carde JP, Schantz ML, Schantz R. A ubiquitous plant housekeeping gene, PAP, encodes a major protein component of bell pepper chromoplasts. Plant Physiol. 1997:**115**(3):1185–1194. https://doi.org/10.1104/pp.115.3.1185

Rao AV, Rao LG. Carotenoids and human health. Pharmacol Res. 2007:**55**(3):207–216. https://doi.org/10.1016/j.phrs.2007.01.012

Rodriguez-Concepcion M, Avalos J, Bonet ML, Boronat A, Gomez-Gomez L, Hornero-Mendez D, Limon MC, Melendez-Martinez AJ, Olmedilla-Alonso B, Palou A, et al. A global perspective on carotenoids: metabolism, biotechnology, and benefits for nutrition and health. Prog Lipid Res. 2018:**70**:62–93. https://doi.org/10.1016/j.plipres.2018.04.004

Schaub P, Rodriguez-Franco M, Cazzonelli CI, Alvarez D, Wust F, Welsch R. Establishment of an Arabidopsis callus system to study

the interrelations of biosynthesis, degradation and accumulation of carotenoids. PLoS One. 2018:**13**(2):e0192158. https://doi.org/10.1371/journal.pone.0192158

Simkin AJ, Gaffe J, Alcaraz JP, Carde JP, Bramley PM, Fraser PD, Kuntz M. Fibrillin influence on plastid ultrastructure and pigment content in tomato fruit. Phytochemistry. 2007:**68**(11):1545–1556. https://doi.org/10.1016/j.phytochem.2007.03.014

Singh DK, McNellis TW. Fibrillin protein function: the tip of the iceberg? Trends Plant Sci. 2011:**16**(8):432–441. https://doi.org/10.1016/j.tplants.2011.03.014

Sun T, Li L. Toward the 'golden' era: the status in uncovering the regulatory control of carotenoid accumulation in plants. Plant Sci. 2020:**290**:110331. https://doi.org/10.1016/j.plantsci.2019.110331

Sun T, Rao S, Zhou X, Li L. Plant carotenoids: recent advances and future perspectives. Mol Hortic. 2022a:**2**(1):3. https://doi.org/10.1186/s43897-022-00023-2

Sun T, Tadmor Y, Li L. Pathways for carotenoid biosynthesis, degradation, and storage. Methods Mol Biol. 2020a:**2083**:3–23. https://doi.org/10.1007/978-1-4939-9952-1_1

Sun T, Wang P, Rao S, et al. (2023) Co-chaperoning of chlorophyll and carotenoid biosynthesis by ORANGE family proteins in plants. Molecular Plant **16**(6):1048–1065. http://dx.doi.org/10.1016/j.molp.2023.05.006

Sun T, Yuan H, Cao H, Yazdani M, Tadmor Y, Li L. Carotenoid metabolism in plants: the role of plastids. Mol Plant. 2018:**11**(1):58–74. https://doi.org/10.1016/j.molp.2017.09.010

Sun T, Yuan H, Chen C, Kadirjan-Kalbach DK, Mazourek M, Osteryoung KW, Li L. OR(His), a natural variant of OR, specifically interacts with plastid division factor ARC3 to regulate chromoplast number and carotenoid accumulation. Mol Plant. 2020b:**13**(6):864–878. https://doi.org/10.1016/j.molp.2020.03.007

Sun T, Zhou F, Huang XQ, Chen WC, Kong MJ, Zhou CF, Zhuang Z, Li L, Lu S. ORANGE Represses chloroplast biogenesis in etiolated Arabidopsis cotyledons via interaction with TCP14. Plant Cell. 2019:**31**(12):2996–3014. https://doi.org/10.1105/tpc.18.00290

Sun T, Zhou X, Rao S, Liu J, Li L. Protein–protein interaction techniques to investigate post-translational regulation of carotenogenesis. Methods Enzymol. 2022b;**671**:301–325. https://doi.org/10.1016/bs.mie.2022.02.001

Sun T, Zhu Q, Wei Z, Owens LA, Fish T, Kim H, Thannhauser TW, Cahoon EB, Li L. Multi-strategy engineering greatly enhances provitamin A carotenoid accumulation and stability in Arabidopsis seeds. aBIOTECH. 2021:**2**(3):191–214. https://doi.org/10.1007/s42994-021-00046-1

Toledo-Ortiz G, Huq E, Rodriguez-Concepcion M. Direct regulation of phytoene synthase gene expression and carotenoid biosynthesis by phytochrome-interacting factors. Proc Natl Acad Sci U S A. 2010:**107**(25):11626–11631. https://doi.org/10.1073/pnas.0914428107

Torres-Romero D, Gomez-Zambrano A, Serrato AJ, Sahrawy M, Merida A. Arabidopsis fibrillin 1-2 subfamily members exert their functions via specific protein-protein interactions. J Exp Bot. 2022:**73**(3):903–914. https://doi.org/10.1093/jxb/erab452

Tzuri G, Zhou X, Chayut N, Yuan H, Portnoy V, Meir A, Sa'ar U, Baumkoler F, Mazourek M, Lewinsohn E, et al. A 'golden' SNP in *CmOr* governs the fruit flesh color of melon (*Cucumis melo*). Plant J. 2015:**82**(2):267–279. https://doi.org/10.1111/tpj.12814

Vainstein A, Halevy AH, Smirra I, Vishnevetsky M. Chromoplast biogenesis in *Cucumis sativus* corollas (rapid effect of gibberellin A3 on the accumulation of a chromoplast-specific carotenoid-associated protein). Plant Physiol. 1994:**104**(2):321–326. https://doi.org/10.1104/pp.104.2.321

van Wijk KJ, Kessler F. Plastoglobuli: plastid microcompartments with integrated functions in metabolism, plastid developmental transitions, and environmental adaptation. Annu Rev Plant Biol. 2017:**68**(1):253–289. https://doi.org/10.1146/annurev-arplant-043015-111737

Vishnevetsky M. Carotenoid sequestration in plants: the role of carotenoid-associated proteins. Trends Plant Sci. 1999:**4**(6):232–235. https://doi.org/10.1016/S1360-1385(99)01414-4

Vishnevetsky M, Ovadis M, Itzhaki H, Levy M, Libal-Weksler Y, Adam Z, Vainstein A. Molecular cloning of a carotenoid-associated protein from *Cucumis sativus* corollas: homologous genes involved in carotenoid sequestration in chromoplasts. Plant J. 1996:**10**(6):1111–1118. https://doi.org/10.1046/j.1365-313X.1996.10061111.x

Walter MH, Strack D. Carotenoids and their cleavage products: biosynthesis and functions. Nat Prod Rep. 2011:**28**(4):663–692. https://doi.org/10.1039/c0np00036a

Wang YQ, Yang Y, Fei Z, Yuan H, Fish T, Thannhauser TW, Mazourek M, Kochian LV, Wang X, Li L. Proteomic analysis of chromoplasts from six crop species reveals insights into chromoplast function and development. J Exp Bot. 2013:**64**(4):949–961. https://doi.org/10.1093/jxb/ers375

Welsch R, Zhou X, Yuan H, Alvarez D, Sun T, Schlossarek D, Yang Y, Shen G, Zhang H, Rodriguez-Concepcion M, et al. Clp protease and OR directly control the proteostasis of phytoene synthase, the crucial enzyme for carotenoid biosynthesis in Arabidopsis. Mol Plant. 2018:**11**(1):149–162. https://doi.org/10.1016/j.molp.2017.11.003

Yang Y, Thannhauser TW, Li L, Zhang S. Development of an integrated approach for evaluation of 2-D gel image analysis: impact of multiple proteins in single spots on comparative proteomics in conventional 2-D gel/MALDI workflow. Electrophoresis. 2007:**28**(12):2080–2094. https://doi.org/10.1002/elps.200600524

Yazdani M, Sun Z, Yuan H, Zeng S, Thannhauser TW, Vrebalov J, Ma Q, Xu Y, Fei Z, Van Eck J, et al. Ectopic expression of ORANGE promotes carotenoid accumulation and fruit development in tomato. Plant Biotechnol J. 2019:**17**(1):33–49. https://doi.org/10.1111/pbi.12945

Yuan H, Owsiany K, Sheeja TE, Zhou X, Rodriguez C, Li Y, Welsch R, Chayut N, Yang Y, Thannhauser TW, et al. A single amino acid substitution in an ORANGE protein promotes carotenoid overaccumulation in Arabidopsis. Plant Physiol. 2015a:**169**(1):421–431. https://doi.org/10.1104/pp.15.00971

Yuan H, Pawlowski EG, Yang Y, Sun T, Thannhauser TW, Mazourek M, Schnell D, Li L. Arabidopsis ORANGE protein regulates plastid pre-protein import through interacting with tic proteins. J Exp Bot. 2021:**72**(4):1059–1072. https://doi.org/10.1093/jxb/eraa528

Yuan H, Zhang J, Nageswaran D, Li L. Carotenoid metabolism and regulation in horticultural crops. Hortic Res. 2015b:**2**(1):15036. https://doi.org/10.1038/hortres.2015.36

Zeng Y, Du J, Wang L, Pan Z, Xu Q, Xiao S, Deng X. A comprehensive analysis of chromoplast differentiation reveals complex protein changes associated with plastoglobule biogenesis and remodeling of protein systems in sweet orange flesh. Plant Physiol. 2015:**168**(4):1648–1665. https://doi.org/10.1104/pp.15.00645

Zhou X, Rao S, Wrightstone E, Sun T, Lui ACW, Welsch R, Li L. Phytoene synthase: the key rate-limiting enzyme of carotenoid biosynthesis in plants. Front Plant Sci. 2022;**13:**884720. https://doi.org/10.3389/fpls.2022.884720

Zhou X, Welsch R, Yang Y, Alvarez D, Riediger M, Yuan H, Fish T, Liu J, Thannhauser TW, Li L. Arabidopsis OR proteins are the major posttranscriptional regulators of phytoene synthase in controlling carotenoid biosynthesis. Proc Natl Acad Sci U S A. 2015:**112**(11):3558–3563. https://doi.org/10.1073/pnas.1420831112

Zhu K, Sun Q, Chen H, Mei X, Lu S, Ye J, Chai L, Xu Q, Deng X. Ethylene activation of carotenoid biosynthesis by a novel transcription factor CsERF061. J Exp Bot. 2021:**72**(8):3137–3154. https://doi.org/10.1093/jxb/erab047